CHAPTER 4

A HYBRID-CASCADED ITERATIVE FRAMEWORK FOR PET AND SPECT IMAGE RECONSTRUCTION

In this chapter, we have discussed the major drawbacks associated with statistical iterative reconstruction algorithms which include the problem of slow convergence, choice of optimum initial point and ill-posedness. To alleviate these issues, three different hybrid cascaded frameworks based on statistical iterative reconstruction algorithms (e.g. MLEM, MRP, and OSEM) have been proposed for PET and SPECT imaging modalities. Their performances are evaluated on computer generated test phantoms and standard thorax real test image. The obtained results are compared with those of previously reported methods. It is observed that the proposed methods perform better in terms of visual image quality and detail preservation.

Rest of the work is organized as follows: Section 4.1, present the introduction of statistical iterative methods with their advantages and limitations. Section 4.2 presents the theoretical background of the proposed framework, Section 4.3 and their subs-sections, presents the proposed methods and model; Section 4.4, presents the results and discussions. Finally presents the conclusion of the work. Finally the overall comparisons of the proposed framework with common datasets used in this thesis are stated in section 4.5.

4.1 Introduction

Today, a wide range of different medical imaging modalities can be found in radiology. These modalities allow the radiologist to view, usually three dimensional, the internal structures of the human body for investigating accurate functional and anatomical information in a non-invasive way. The use of various non-invasive techniques (Marcel Beister et. al., 2012) has greatly reduced risks to patients and has increased our understanding of how the body works.

SIR method have shown great potential to replace traditional analytical methods like FBP which take into account of statistical properties of the data have been shown to be superior in suppressing noise and streak artifacts. Statistical iterative reconstruction (SIR) (Qi J *et. al.*, 2006) methods reconstruct images by iteratively maximizing likelihood function. Examples are MLEM (Shepp and Vardi, 1982), Median Root Prior (MRP) (Green PJ *et. al.*, 1990), Ordered Subsets Expectation Maximization (OSEM) (Hudson and Larkin, 1994) and their variants (Xu Lei *et. al.*, 2007). It plays an important role on the quality of the images produced by PET/SPECT since they can perform better with noisy, incomplete data, accurate system modeling, image prior knowledge, and as an alternative to both the analytical and algebraic methods, being less sensitive to noise and sparse view inputs. However, the major drawbacks associated with statistical algorithms are their slow convergence, the choice of an optimum initial point, and ill-posedness.

Nowadays, OSEM (Ordered Subset Expectation Maximization) has become the most widely used iterative methods in Emission computed tomography (ECT) (Jinyi Qi et. al., 2006). Image reconstruction algorithms play a significant role in many ECT devices. In order to obtain a high quality reconstructed images from the collected projection data, an excellent image reconstruction algorithm is needed. ECT image quality is dependent on a number of parameters in the acquisition of the projectional raw data, such as the intrinsic resolution of the camera, choice of collimator, geometry of the gantry set-up, timing of the study acquisition, and patient-derived factors such as body habitus and movement during study acquisition (Jinyi Qi et. al., 2006). ECT produces an accurate measure of spatial distribution of radioactive substances throughout the patient to extract

physiological or functional information. The rate of radioactive emissions can best be described by a Poisson process (Rajeev Srivastava et. al., 2013). Therefore, the noise properties of emission tomography are also spatial-variant in nature. (Hudson and Larkin, 1994) proposed an alternative version of maximum likelihood approach called OSEM and it is widely used by modern ECT clinical scanners together with MLEM. They showed that their refinements accelerate the iteration process by a factor proportional to the number of subsets. But, the quality of the reconstructed image with OSEM still remains same as MLEM and it also suffers from the problem of initialization and ill-posedness. So, there has to be an optimum starting point and optimum stopping rules are needed, which stops the reconstruction process well in time before we over run the algorithm as well as to maintain the visual quality of the reconstructed images. In this work, we continue the discussion on the solution of these problems.

Firstly, the discussion related to selection of an optimum initial point which affects the above stated problems directly. The initialization of the algorithm can have a great influence on the final solution of the reconstructed image. By choosing the right point for the algorithm one can avoid the case of running into stagnation. If the chosen point is closer to the best result, then the algorithm will have to put lesser effort into reaching to the result and the same number of iterations will yield a better looking image. Also, while choosing the initial image as any random collection of pixels, we might run away from the desired result and reconstruction might not be able to reproduce the desired image. In such cases, the image will contain patches of noisy areas. Secondly, the issue related to ill-posedness nature of iterative algorithms, which can be tuned to a well-posed by using suitable regularization term. To incorporate a suitable regularization term within a reconstruction framework is to control the noise propagation and to produce a reasonable reconstruction. The most common widespread regularization techniques are available in (Quan Zhang et. al., 2013; Qian He et. al., 2014; Zhu Hl et. al., 2006).

Here, in figure 4.1 presents, a new Generalized Hybrid-Cascaded Framework for PET/SPECT Image Reconstruction. The proposed frameworks reduce the number of iterations as well as improve the quality of reconstructed. This method speeds up the process by using a fast reconstruction algorithm first and

then switches to a slower but more precise algorithm. Additionally, regularization term anisotropic diffusion proposed by Perona and Malik (Perona and Malik, 1990) is combined to maximize the likelihood function. The proposed method solves computational time, slow convergence as well as ill-conditioned problem of SIR methods. Numerical simulation experience demonstrates that proposed hybrid cascaded reconstruction algorithm is superior in performance to the MLEM, MRP, OSEM or SART alone as well as other state-of the- art hybrid iterative reconstruction methods available in literature.

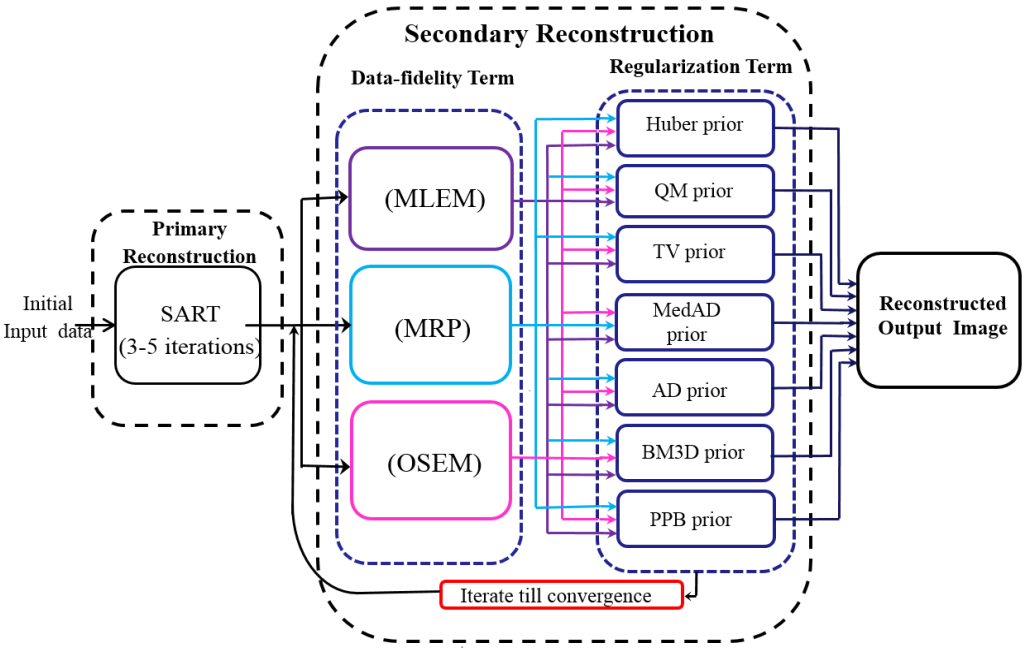

Fig. 4.1: Generalized Hybrid-Cascaded Framework for PET/SPECT Image Reconstruction

To address above mentioned issues of initialization and ill-posedness, in this work, an efficient hybrid-cascaded framework is proposed for improving the quality of SPECT/PET images. This framework consists of breaking the reconstruction process into two parts viz. primary and secondary. Primary and secondary reconstruction parts work in a cascaded manner. Output from primary reconstruction is fed into secondary reconstruction. This allows us to use more than one algorithm for reconstruction and extract the benefits of both. With a cascaded network, we attain performance superior than either of the two algorithms used alone.

4.2 Background

- **Brief discussion about MLEM**

MLEM is one of the most widely used iterative methods for PET/SPECT reconstruction (F. Benvenuto *et. al.*, 2008; Quan Zhang *et. al.*, 2013). MLEM is based on a Poisson model in the image reconstruction process and typically used in conditions that the measured projection data contains a lot of noise due to limited photon statistics. This algorithm computes the maximum-likelihood estimate (ML) of a probability distribution function in a reconstructed image from the measured projection data via an expectation maximization algorithm (EM). The major advantages of SIR based MLEM method is that it has better reconstruction capability, i.e. produces good quality reconstructed image, but is associated with the problem of initialization and slow convergence. In this work, we continue the discussion on the solution of these problems as follows:

First issue related to MLEM algorithm is the initialization of the algorithm and their slow convergence which can have a great influence on the final solution of the problem, as there can be several issues in statistical iterative reconstruction algorithms such as huge computational burden associated with the multiple re-projection and back-projection operation cycles through the image domain, complex physics and noise modeling. The problem of choosing an optimum initial point affects the above stated problems directly. If the chosen point is closer the best result, then the algorithm will have to put lesser effort into reaching to the result and the same number of iterations will yield a better looking image. Also, while choosing the initial image as any random collection of pixels, we might run away from the desired result and reconstruction might not be able to reproduce the desired image. In such cases, the image will contain patches of noisy areas.

A second major issue related to the ill-posedness. During reconstruction process, Poisson noise effectively degrades the quality of reconstructed image. However, it can be tuned to a well-posed problem by means of regularization. Regularization means the use of some additional function in such a way that the final image is a compromise between the data and the object as it is expressed by the regularization function. To incorporate a suitable regularization term

within a reconstruction framework is to control the noise propagation and to produce a reasonable reconstruction. Numerous edge preserving priors have been proposed in the literature (Chen Y *et. al*., 2006; Lange K *et.al.*, 1990; Denisova NV *et.al.*, 2004; Chlewicki W *et. al.,* 2004; Panin VY *et. al.*, 1999; Perona and Malik, 1990; Rajeev Srivastava *et. al.*, 2013; Liang Z *et. al.*, 1989; Nunez J *et. al.*, 1990; Fessler, 2006; Herman and Levitan, 1987; Chen G-H *et. al.*, 2008; Chun I Y *et. al.*, 2013; Kang D *et. al*. 2013; Wang G *et. al.*, 2012; Z. G. Gui *et. al.*, 2012; D. Kazantsev *et. al.*, 2012) to produce sharp edges while suppressing noise within boundaries. The most common widespread regularization techniques are penalized-likelihood reconstruction algorithm (Jun Ma, 2010), or maximum-a-posteriori reconstruction (MAP) (Herman and Levitan, 1987), and the one-step-late algorithm (Green PJ *et. al.*, 1990) used to reduce noise effect and preserving the edges. A median root prior (MRP) is to encourage preservation of the piecewise contrast region while eliminating impulsive noise, but reconstructed images still suffer from streaking artifacts and Poisson noise. Work in this direction in the context of PET/SPECT has focused primarily on modifications and improvements of MLEM with different regularization terms (Chung Chan *et. al.*, 2009).

To maximum a posterior (MAP) estimator, the reconstructed image can be obtained by maximizing the log-likelihood function *L(f),* i.e.,

$$L(f) = \arg\max_{f \geq 0} L(f) \qquad (4.1)$$

To solve the optimization problem of iterative methods given by Eq. (4.1), (Shepp and Vardi, 1982) proposed the MLEM algorithm, and the iterative formula can be described as follows:

$$f_j^{k+1} = \frac{f_j^k}{\sum_{i=1}^{I} a_{ij}} \sum_{i=1}^{I} \frac{a_{ij} y_i}{\sum_{l=1}^{J} a_{il} f_l^k} \quad for\ j = 1, 2, \ldots, N. \qquad (4.2)$$

Although MLEM algorithm is better than filtered back-projection (FBP) algorithm (Zeng GL *et. al.*, 2013), its major problem is that different features converge at different speeds, and as the number of iteration increases, they tend to computationally intensive. Additionally, MLEM algorithm is also ill-posed. To deal with the slow convergence and speed problem of MLEM, Ordered subsets EM (OSE M) (Hudson and Larkin, 1994) algorithm was proposed which is a

successful approach. However, a drawback of OSEM is that, the reconstructed results still suffer from noise artifacts.The slow convergence and speed issues related to MLEM can also be effectively handled with efficient implementations which make use of advanced programming techniques (William H *et. al.,* 1992). Rigorous mathematical analysis in the case of Landweber iterations and conjugate gradient is given in (Per Christian Hansen, & Maria Saxild-Hansen, 2012) for solving EM based iterative methods. Other alternative optimization approaches to estimating the ML solution is available in literature. For example, the use of complex conjugate gradient (Guobao Wang *et. al.,* 2012), gradient descent optimization (R. Salakhutdinov *et. al.,* 2003), grouped coordinate ascent, and fast-gradient based Bayesian reconstruction methods (Erkan U. Mumcuoglu *et. al.,* 1994) etc., which have shown fast convergence rates (G I Angelis *et. al.,* 2011). A number of examples of the same behavior are also discussed in (Emran M Abu Anas *et. al.,* 2011).

- **Brief discussion about MRP**

Although MLEM algorithm is better than filtered back-projection (FBP) algorithm (J. Devaney, 1982), its major problem is that different features converges at different speeds, and as the number of iteration increases, the reconstructed results suffer from noise artifacts. Median root prior (Green PJ *et. al.,* 1990) is a successful approach to accelerate the MLEM algorithm and solve the slow convergence issue. However, a drawback of MRP is that, the reconstructed results suffer from noise artifacts. The usual method to solve this problem is to introduce a regularization term, the objective function is:

$$\hat{f} = \arg\max_{f \geq 0} L(f) + \ln P(f) \qquad (4.3)$$

where $\hat{f}$ is the MAP estimate of the radiotracer distribution, *L(f)* is the log likelihood and *P(f)* is the prior probability density. The posterior probability *P(g| f)* can be maximized by the one-step-late (OSL) iterative procedure proposed by (Green PJ *et. al.,* 1990).

$$f_j^{k+1} = \frac{f_j^k}{\sum_i a_{ij} + \beta \frac{\partial}{\partial f_i U\left(f_j^k\right)}} \sum_i \frac{g_i}{\sum_{i'} a_{i'j} f_{i'}^k} \qquad (4.4)$$

where $f_j^{(k+1)}$ is the updated image after *(k+1)th* iteration, g_i is the projection data from different angles available to us and a_{ij} is the weight matrix which describes the transition law between the measured projection data and the estimated image vector. It fully depends on the geometrical characteristics of the PET/SPECT scanner. In Eq. 4.4, $U(\cdot)$ is the energy function and β is the Bayes weight of the prior. The image is reconstructed by iteratively updating Eq. (4.4) to reach at least a local maximum. The MRP can be incorporated into the OSL formula by replacing the derivative of the prior function with a relative form of the smoothing prior (Alenius S, Ruotsalainen, 2002):

$$f_j^{k+1} = \frac{f_j^k}{\sum_i a_{ij} + \beta \dfrac{f_j^k - M\left(f_j^k\right)}{M\left(f_j^k\right)}} \sum_i \frac{g_i}{\sum_{i'} a_{i'j} f_{i'}^k} \tag{4.5}$$

where $M\left(f_j^k\right)$ is the median of pixel *j* within its neighborhood. MRP is a Bayesian based statistical estimation method whereas SART is algebraic estimation based reconstruction process. Due to the probabilistic nature of positron emission tomography PET (D.L.Bailey *et. al.*, 2005), MRP is more suited for the image reconstruction technique. It can accommodate the nature of photon reception in detectors and hence leads to better estimation of projections. However, the images reconstructed by MRP are still noisy because median filter cannot remove Gaussian and Poisson noise effectively, which dominate in PET images (F. Benvenuto *et. al.*, 2008).This method also suffers from optimal point initialization and slow convergence.

- **Brief discussion about OSEM**

Hudson and Larkin (Hudson et. al.. 1994) proposed an alternative algorithm to MLEM that processed the data in subsets within each iteration. They showed that their method accelerated the iteration process by a factor proportional to the number of subsets. This algorithm was named as Ordered Subsets Expectation Maximization (OSEM) and it is widely used by modern PET clinical scanners together with MLEM. In the OSEM algorithm the projection data are grouped into *Ordered Subsets* (OS). The number of these subsets defines the OS level.

Detailed desctiption of OSEM algorithms with their advantages and limitations are discussed in Chapter 2, section 2.3.2.2 statistical methods.

- **Brief discussion about SART**

In the following section, a brief discussion about the SART reconstruction algorithm is given that is used as a primary part of the proposed framework. SART is a particular instance of algebraic reconstruction methods designed to solve the linear system in image reconstruction. These methods pose the problem of reconstruction from projections as a set of simultaneous equations:

$$Ax = p, \tag{4.6}$$

where A is an $M \times N$ design matrix with weights a_{ij}, x is the sought-after N dimensional image vector, and p is an M-dimensional column vector containing the observed projection values. That is, M is the number of rays, N is the number of image cells, and the weight a_{ij} gives the contribution of the j^{th} cell to the ray sum along the i^{th} ray. Various iterative algebraic algorithms have been proposed to solve Eq. (7) (Gordon R *et. al.,* 1970; Kaczmarz S *et al.*, 1937; Gilbert *et al.*, 1972; Andersen *et al.,* 1994; Fernández J *et al.,* 2002; R. Vijayarajan *et al.*, 2014; Marcel Beister *et al.,* 2012; Guan H *et al.,* 1998). SART has been proven to be the most useful iterative reconstruction technique (Ming, J *et al.,* 2003) and better suited for real time applications. SART is characterized by better robustness than ART under noise and its convergence speed is reported to be faster than other algebraic iterative methods (Wang G *et al.,* 2004). The major advantage of SART is that, even in high resolution tomographic problems, number of unknowns can be solved with less computational load. (Hobiger *et al.* 2008) proved that SART iterative approach converges to a solution such that the error is minimized. (Michael *et. al.,* 2014) mentioned that SART has the advantage that it always iterates to converge to a unique solution irrespective of the above situations. No further study has been reported yet to verify this statement.

Typically, the SART algorithm begins with an arbitrary $X_{(0)}$ and then begins to iterate until they are the correct ones. It is possible that the arbitrary initial value will greatly deviate from the true value. So the number of iterations can be very large. Consequently, the initial solution $X_{(0)}$ is defined by

$$x_j^k = x_j^{k-1} + \frac{\lambda}{\sum_{P_i \in P_\varphi} p_{ij}} \sum_{P_i \in P_\varphi} \left(\frac{P_i - \sum_{n=1}^{N} p_{in} x_n^k}{\sum_{n=1}^{N} p_{in}} p_{ij} \right) \tag{4.7}$$

where P_φ represents the projection view at angle φ, and λ is known as the relaxation parameter, and N is the total number of pixels. The process of iteration first guesses the values of the pixels and then alters these values until it is correct one. All the equations belonging to the same angle at the same time $\left(P_i \in P_\varphi\right)$ are used before comparing the new values of the pixels with the old one. Furthermore, it has been pointed out that SART can be improved by adjusting the relaxation parameters (Michael *et. al.,* 2014). Careful selections for the relaxation parameters can lead to the better qualities of reconstructions (Ming, J *et al.,* 2003; Wang G *et al.,* 2004; Hobiger *et al.* 2008; Michael *et. al.,* 2014). Here, we choose the value of λ as less than one, and find good convergence with small number of iterations. In each iteration of SART, all the pixels with the same weights receive the same corrections even they have different gray levels. The rate of convergence of a SART based reconstruction approach is faster, but the quality of reconstructed image is not better with respect to MLEM approach.

4.3 Proposed Models

This section presents, three different hybrid cascaded framework based on statistical iterative reconstruction algorithms (e.g. MLEM, MRP, and OSEM) have been proposed for PET and SPECT imaging modalities. Their performances are evaluated on computer generated test phantoms and standard thorax real test image. The obtained results are compared with those of previously reported methods. It is observed that the proposed methods perform better in terms of visual image quality and detail preservation. For quantitative analysis, various performance measures such as: SNR, PSNR, RMSE, CP, MSSIM are used.

4.3.1 MLEM based hybrid-cascaded framework for PET and SPECT image Reconstruction Algorithm

PET and SPECT are effective and indispensable imaging tools for the application of medical image reconstruction. Statistical iterative methods for image reconstruction like Maximum Likelihood Expectation Maximization (MLEM)

play a significant role in the quality of the images produced by PET/SPECT and allow for accurately modeling the counting statistics and the photon transport during acquisition as reported in literature. The major drawbacks associated with this algorithm include the problem of slow convergence, choice of optimum initial point and ill-posedness. In this work, an efficient hybrid-cascaded iterative framework for MLEM approach is proposed to alleviate these limitations. This framework consists of breaking the reconstruction process into two parts viz. primary and secondary. During primary part, simultaneous algebraic reconstruction technique (SART) is applied to overcome the problems of slow convergence and initialization. It provides fast convergence and produce good reconstruction results with lesser number of iterations than other iterative methods. The task of primary part is to provide an enhanced image to secondary part to be used as an initial estimate for reconstruction process. The secondary part is a hybrid combination of two parts namely the reconstruction part and the prior part. The reconstruction is done using MLEM algorithm while median anisotropic diffusion (MedAD) filter is used as prior to deal with ill-posedness. The comparative analysis of the proposed method with other standard methods existing in literature is presented for four different test phantoms both qualitatively and quantitatively. Using cascaded primary and secondary reconstruction steps, yields significant improvements in reconstructed image quality. It also accelerates the convergence and provides enhanced results using the projection data. The obtained results justify the applicability of the proposed method.

4.3.1.1 Proposed Method and Model

The proposed hybrid model consists of two parts namely primary reconstruction and secondary reconstruction as shown in Fig.4.2. A detailed description of the proposed model as follows:

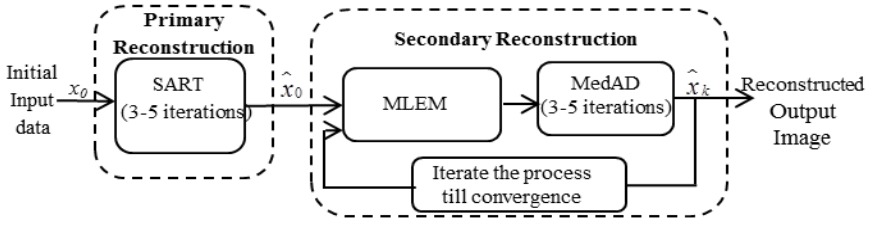

Fig. 4.2: Proposed MLEM based hybrid-cascaded framework (Model-1)

- ***Primary Reconstruction***

During primary part, SART is used as initialization stage for MLEM i.e. SART image is used for the initial condition in MLEM (the initial value of each pixel) for the following reasons: it is presumably close to the final optimized solution (lessening the need for iterations); it is a valid indicator of specific-slice image noise; and in second step it can be quickly obtained. For modelling and use of iterative reconstruction, minimum convergence is achievable with the MLEM reconstruction and median anisotropic diffusion (MedAD) (Ling and Bovik, 2002) as regularization term with MLEM algorithm to reduce noise levels and enhances the visual quality of images. In particular, choosing a suitable initial value for the MLEM algorithm in such a manner to remove the noise or error as well as improvised the slow convergence problem significantly.

The Poisson noise encountered in image PET/SPECT data falls under multiplicative noise. This noise type is also called shot noise and is closely related to Gaussian noise (F. Benvenuto *et al.,* 2008). SART finds the Euclidian distance between calculated projections and true projections and thus reduces the weighted least squared error. The error correcting term in SART is also additive in nature (Zeng GL. *et al.,* 2013). MLEM uses multiplicative ways to find and back project error in projections during reconstruction and thus is better suited for Poisson noise. We need to introduce non-negativity constraints for SART technique hence we only need to ensure that initial image is positive (system matrix is always positive).

It is well established in literature that the SART based reconstruction approaches converges faster than MLEM but the only drawback of SART is that the quality of reconstructed images produced by it are inferior to MLEM based approaches. Hence, in this work we exploit the advantage of faster convergence of SART and incorporate it in our hybrid approach during primary reconstruction to accelerate the MLEM and deal with the problem of initialization. Here, in this work we use first, 3-5 iterations of SART to produce the initial estimate of the image which acts as the input to the MLEM in secondary reconstruction phase of our proposed model.

Hence, the mathematical model for primary reconstruction phase of the proposed model is given as follows by re-writing Eq. no (4.7):

$$x_{SART,j}^{k} = x_{j}^{k-1} + \frac{\lambda}{\sum_{i=1}^{N} p_{ij}} \sum_{i=1}^{N} \left(\frac{e_{j}^{k}}{\sum_{j=1}^{M} p_{ij}} p_{ij} \right) \tag{4.8}$$

where M is the total number of rays and N is the total number of pixels. λ is the relaxation parameter and error (e_j^k)is calculated in projections using $e_j^k = P_j - p_j^k$,where P_j is true projections and p_j^k is calculated projections at k^{th} iteration.

- ***Secondary Reconstruction***

The secondary reconstruction is a hybrid combination of iterative reconstruction and a prior part as shown in Fig. 4.2. They both work in conjunction to provide one iterative cycle of secondary reconstruction. This is repeated a number of times till we get the required result. The use of prior knowledge within the secondary reconstruction enables us to tackle noise at every step of reconstruction and hence noise is tackled in an efficient manner. Using median anisotropic diffusion (MedAD) (Ling and Bovik, 2002) inside reconstruction part gives better results than working after the reconstruction is over. The basic idea of MedAD is to choose a diffusion coefficient in different diffusion region so that regions are smoothed out and edges are preserved. With this hybrid-cascaded framework, the problem of slow convergence, choice of optimum initial point and ill-posedness of MLEM algorithm are tackled in a much better and efficient manner. The convergence is speeded up and output results enhanced to an appreciable amount with very less expense in computational complexity.

In secondary reconstruction phase of the proposed model, the output obtained in primary reconstruction phase is used as the initial input to the MLEM i.e. the output of the k^{th} SART iteration given by Eq. (4.5) is used as an initial iteration of MLEM and then updating the reconstructed images by n^{th} projections. After the initialization, the MLEM in secondary phase iteratively produces the final reconstructed image. Hence the modified MLEM method reads as follows:

Initial value: $f_j^{(0)} = x_{SART,j}^{(k)}$, (4.6a)

$$f_j^{(n+1)} = f_j^{(n)} \left(\frac{1}{\sum_{i=1}^{I} a_{ij}} \sum_{i=1}^{I} \frac{a_{ij} y_i}{\sum_{l=1}^{J} a_{il} f_l^n} \right), \quad (4.6b)$$

where $f_j^{(n+1)}$ is the value of pixel *j* after the nth iteration of MLEM correction step.

Although likelihood increases, the images reconstructed by modified MLEM (initialized by SART, i.e. SART+MLEM) are still noisy because of ill-posed nature of iterative reconstruction algorithms. The anisotropic diffusion (AD) is an iterative 'tunable' nonlinear partial differential equation (PDE) based diffusion prior introduced by (Perona and Malik, 1990) for noise removal was recently introduced into tomography reconstruction that purports to filter the noise without blurring edges. Overcoming the undesirable effects of linear smoothing filter, such as blurring or dislocating the useful edge information of the images, AD and its variant has been widely used in image smoothing, image reconstruction and image segmentation (Qian He et. al., 2014; Kazantsev D et. al., 2012; Zhiguo Gui et. al., 2012; Rajeev et. al., 2013). The basic equation is:

$$\frac{\partial f}{\partial t} = div\left[C(\nabla f) \nabla f \right] \quad (4.7)$$

where *f* is the image , *t* is the iteration step, ∇f is the local image gradient and $C(\nabla f)$ is the *diffusion function*, which is a monotonically decreasing function of the image gradient magnitude, sometimes called the 'edge-preserving' function. The following *diffusion functions* were first proposed by (Perona and Malik, 1990):

$$C_1(f) = \exp\left[-\left(\frac{\nabla f}{K} \right)^2 \right] \quad \text{or} \quad C_2(f) = 1 \Big/ 1 + \left(\frac{|\nabla f|}{K} \right)^2 \quad (4.8)$$

where *K* is a gradient threshold that controls the edge sensitivity of the model. It is a user-specified constant which determines the threshold of the local gradients and controls the edge sensitivity of the filter. However, P-M diffusion model can remove isolated noise and preserve the edges to some extent it cannot preserve the edge details effectively and accurately. To address the limitation of AD

method, here we use median filter to the result obtained by AD method (Ling and Bovik, 2002) (abbreviated as: MedAD) in each iteration and the discretised form of the proposed MedAD based model using finite difference schemes (William H. Press *et al.*, 1992) is given as follows:

$$f_j^{k+1} = f_j^k + \Delta t \sum_{j' \in N_j} \left(C\left(\left| \nabla f_{j,j'}^k \right| \right) \nabla f_{j,j'}^k \right) \tag{4.9}$$

$$f_{j+1}^{k+1} = Median\left(f_j^{k+1}, W \right) \tag{4.10}$$

For the discretized versions of Eq. (4.9) to be stable, the von Neumann analysis (William H. Press *et al.*, 1992) shows that we require $\Delta t/(\Delta x)^2 \leq 1/4$. The value of $\Delta t \leq 1/4$ when $\Delta x = 1$, where Δx is the spacing between the raster grid size of the image *f(x, y)* in x-direction. Therefore, the value of Δt is set to $1/4$ for stability of Eq. (4.9), and *W* in Eq. (4.10), is the window size for the median operator (such as a 3×3 square).

Towards the end, we refer to the proposed algorithm as an efficient hybrid approach for PET/SPECT image reconstruction and outline it as follows.

- **The Proposed Algorithm**

(A) Initialize image using SART algorithm

Let the following symbols be used in the step 1 of the algorithm:

X = true projections,

p_{ij} = system matrix,

y^k = updated image after k^{th} iteration of SART,

x_j^k = calculated projections at k^{th} iteration.

1. Set k = 0 and chose any random image (zero image density or random image density).

2. Calculate Projections: find projections after k^{th} iterations using updated image

$$x_j^k = p_j^T * y_i^{(k)} \tag{4.11}$$

3. Calculate Error:-Find error in calculated projection using

$$e_j^k = X_j - x_j^k \tag{4.12}$$

4. Back Projection:- update the image after iteration k

$$y_i^{(k+1)} = y_i^{(k)} + \frac{\sum_j p_{ij} * \frac{e_j^k}{\sum_{i=1}^{N} p_{ij}}}{\sum_j p_{ij}} \tag{4.13}$$

5. Put k = k+1, repeat for 3-5 iterations. Obtain the final image y_{final} .

(B) Reconstruction using MLEM algorithm

Let the following symbols be used in the step 2 of the algorithm:

N_{true} = true projections,

G = system matrix,

L^k = updated image after k[th] iteration of SART,

N_{calc}^k = calculated projections at k[th] iteration.

8. Set k = 0 and put

$$L^0 = y_{final} \tag{4.14}$$

Calculate Projections: find projections after k^{th} iterations using updated image

$$N_{calc}^k = G^T * L^k \tag{4.15}$$

9. Error Calculation:-Find error in calculated projection(element-wise division)

$$N_{error}^k = \frac{N_{true}}{N_{calc}^k} \tag{4.16}$$

Back projection:-back project the error onto image

$$X_{error}^k = G * N_{error}^k \tag{4.17}$$

10. Normalization:- normalize the error image(element-wise division)

$$X_{norm}^k = \frac{X_{error}^k}{\sum_j G_{ij}} \tag{4.18}$$

11. Update:- update the image

$$L_m^{k+1} = L^k * X_{norm}^k \tag{4.19}$$

(C) Prior: use median ad as prior

12. Set m = 0 and apply Median Anisotropic Diffusion (abbreviated as: MedAD)

$$L_{m+1}^{k+1} = MedAD\left(L_m^{k+1}\right) \tag{4.20}$$

13. Put m = m+1 and repeat till m = 3;

14. Put k = k+1, repeat with MLEM reconstruction.

In our algorithm, the SNR is monitored during each loop of stage II. The processing is stopped when SNR begins to saturate or degrade from any existing value.

4.3.1.2 Results and Discussions

In this section of the work, results and performance analysis of the proposed method are presented for three different computer generated PET/SPECT phantoms and one standard medical thorax image, both qualitatively and quantitatively. In this simulation study, only two- dimensional (2-D) simulated phantoms were considered. This was because our main aim here is to compare proposed hybrid method with other algorithms and to demonstrate that the proposed method was applicable to different imaging modalities such as PET/SPECT, where 2-D phantoms were sufficient for this purpose. The comparative analysis of the proposed method is also presented with other standard methods available in literature such as MLEM (Shepp and Vardi, 1982), MRP (Green PJ *et. al.*, 1990), OSEM (Hudson and Larkin, 1994), and MLEM+AD (Qian He *et. al.*, 2014). For simulation study MATLAB 2013b software was used on PC with Intel(R) Core (TM) 2 Duo CPU U9600 @ 1.6GHz, 4.00 GB RAM, and 64 bit Operating system. For quantitative analysis the various performance measures used include signal-to-noise ratio (SNR), the root mean square error (RMSE), the peak signal-to-noise ratio (PSNR), the correlation parameter (CP) (Rajeev *et. al.*, 2013), and mean structure similarity index map (MSSIM) (Rajeev *et. al.*, 2013). The SNR, RMSE and PSNR give the error measures in reconstruction process. The correlation parameter is a measure of edge preservation in the reconstructed image. The MSSIM is a measure of preservation of luminance, contrast and structure of the image after the reconstruction process, which is necessary for medical images. The definitions of these quantitative measures are discussed in Chapter 2 section 2.8, performance measures.

For implementation of the proposed method i.e. (SART+MLEM+MedAD) algorithms Eq. (4.5- 4.10) were used. During step 1 of the proposed method which deals with the problem of initialization to

MLEM, SART described by Eq. (4.9) was run for 5-10 iterations and the value of λ was set to 0.0033 for each dataset. Output provided by this step of SART is used as an input to the step 2 of the proposed method. To deal with the problem of ill-posedness of traditional MLEM here in step 2, a hybrid filter as a prior i.e. Median anisotropic diffusion (MedAD) filter was used in each step of the traditional MLEM. In step 2 the MedAD was run for 3 iterations with each MLEM step which is described by Eqs. (4.5 to 4.10). For the implementation of step 2 of the proposed algorithm by Eq. (4.9) the value of Δt was set to 1/7 and 0.25 for three computer generated phantoms and standard medical thorax phantom image respectively. For the computation of diffusion coefficient used by Eq. (4.9) and described by Eq. (4.8), the value of threshold parameter *k* was set to 1/100 and 5 for three computer generated phantoms and standard medical thorax phantom image respectively. The whole algorithm is run for 1000 iterations and graphs are plotted for SNR, RMSE, PSNR, correlation parameter (CP), and MSSIM. This is done to ensure that the algorithm has only single maxima and by stopping at the first instance of stagnation or degradation, we are not missing any further maxima which might give better results. The experiments revealed major observations. The brief description of the three computer generated phantoms and one standard medical thorax phantom image are given as follows: Fig. 4.3, shows the visuals of the test phantoms used for the simulation purposes. These test phantoms are (a) Modified Shepp-Logan phantom (128×128 pixels), (b) PET Test phantom (128×128 pixels), (c) SPECT Test phantom (128×128 pixels), (d) Medical thorax image (128×128 pixels).

(a) (b) (c) (d)

Fig. 4.3: The phantoms used in the simulation study, (a) Modified Shepp-Logan phantom (128×128 pixels), (b) PET Test phantom (128×128 pixels), (c) SPECT Test phantom (128×128 pixels), (d) Medical thorax image (128×128 pixels)

Test case 1:

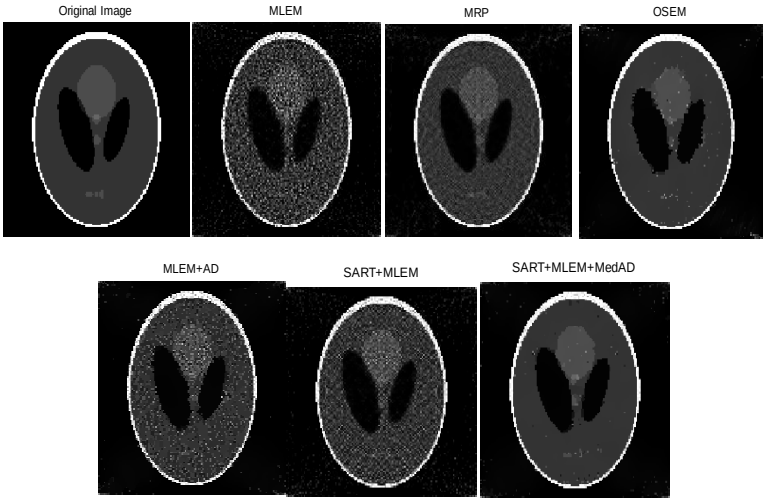

Fig. 4.4: The Modified Shepp-Logan phantom with different reconstruction methods. Projection including 15% uniform Poisson background events.

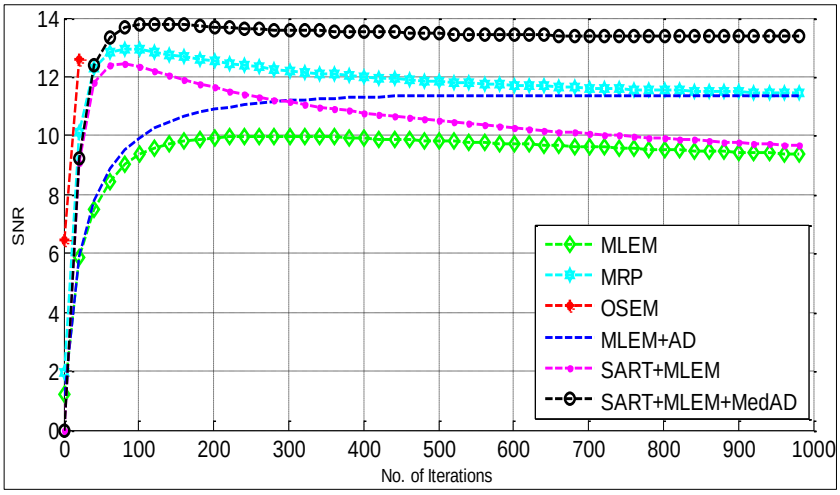

(a)

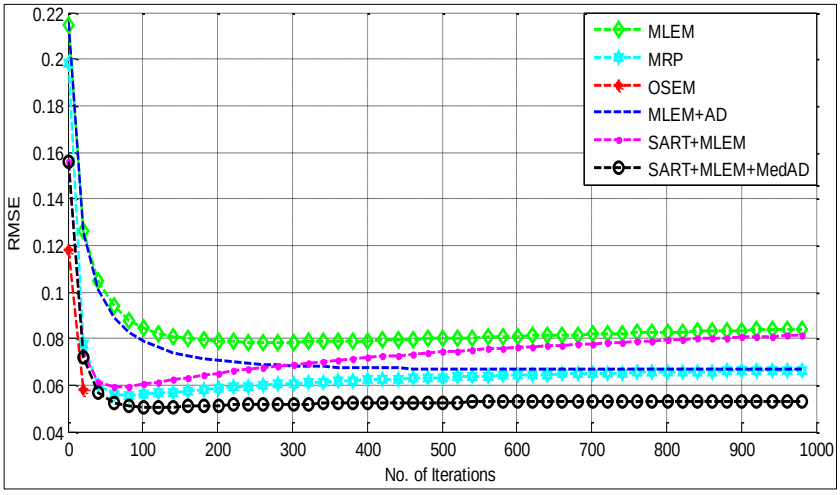

(b)

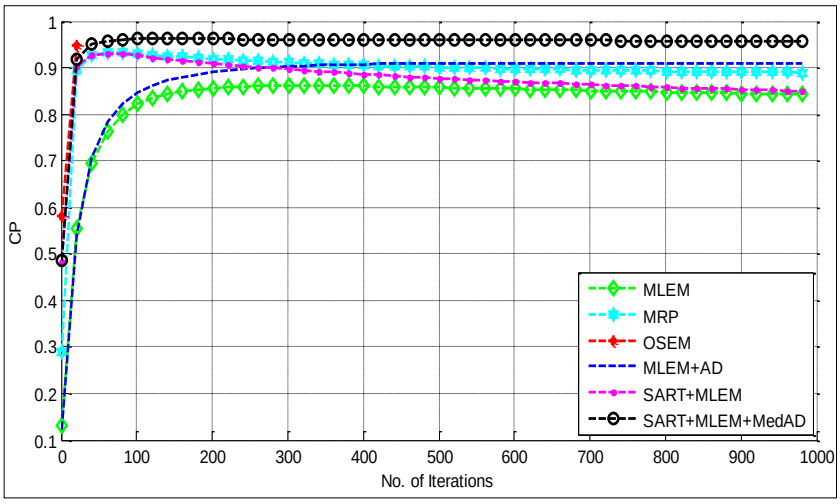

(c)

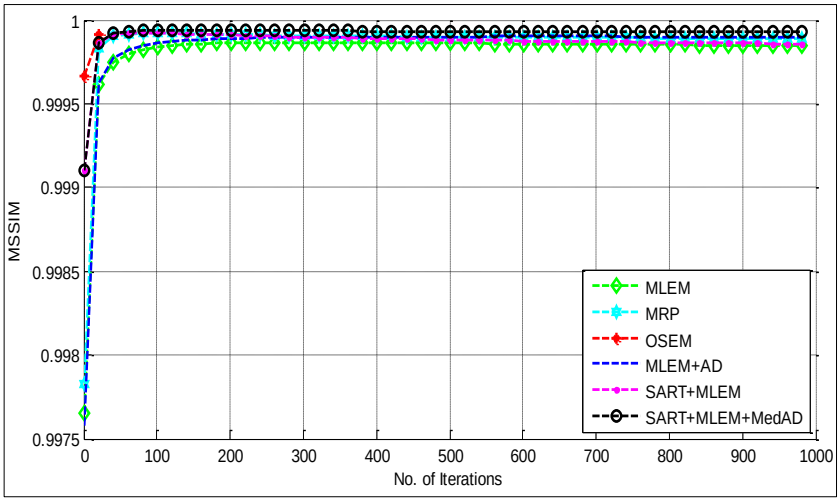

(d)

Fig.4.5: The Plots of (a) SNR, (b) RMSE, (c) CP and (d) MSSIM along with No. of Iterations for different reconstruction algorithms for Test case 1.

Table 4.1: Performance measures for the reconstructed images using Proposed (SART+MLEM+MedAD) and other methods for Test case 1

Performance Measures	MLEM	MRP	OSEM	MLEM+AD	SART+MLEM (Proposed method without prior)	SART+MLEM+MedAD (Final proposed method with prior)
SNR	9.9900	12.9546	12.6123	11.3773	12.4551	13.8022
RMSE	0.0784	0.0557	0.0580	0.0668	0.0590	0.0505
PSNR	70.2792	73.2439	72.9016	71.6665	72.7443	74.0915
CP	0.8611	0.9328	0.9489	0.9102	0.9308	0.9628
MSSIM	0.9997	0.9999	0.9999	0.9999	0.9998	0.9999

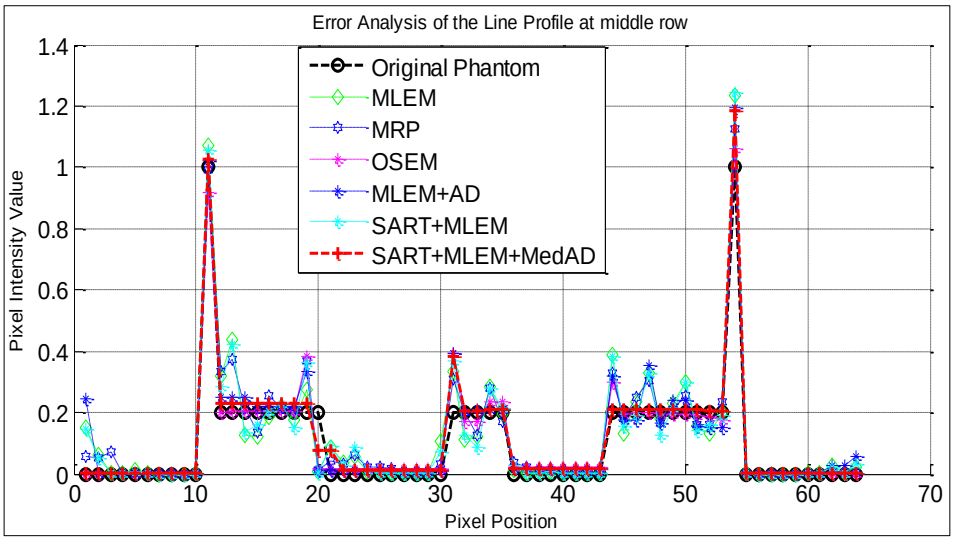

Fig. 4.6: Line Plot of Shepp-Logan head Phantom using proposed method (SART+MLEM+MedAD) with other methods .

Test case 2:

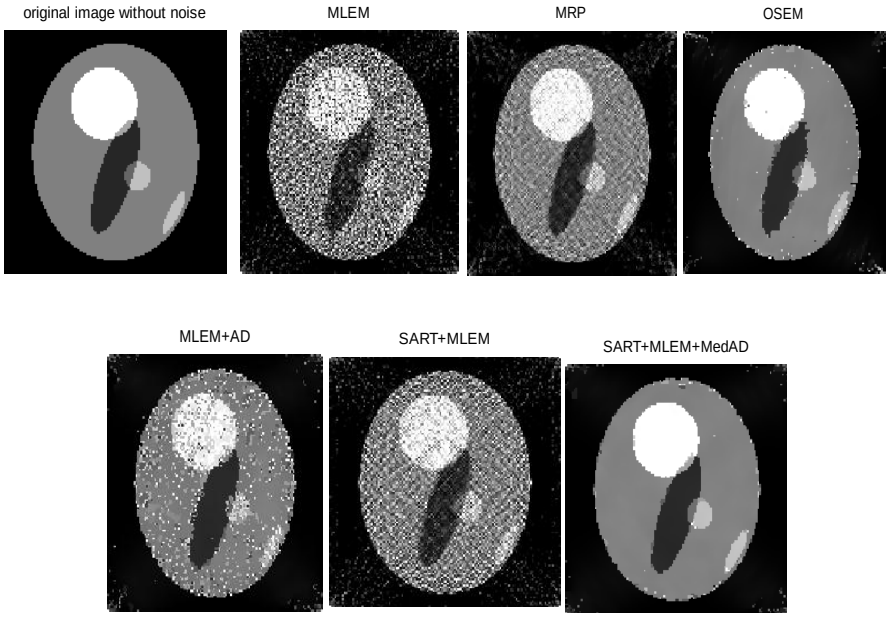

Fig. 4.7: The PET test phantom with different reconstruction methods. Projection including 15% uniform Poisson distributed background events.

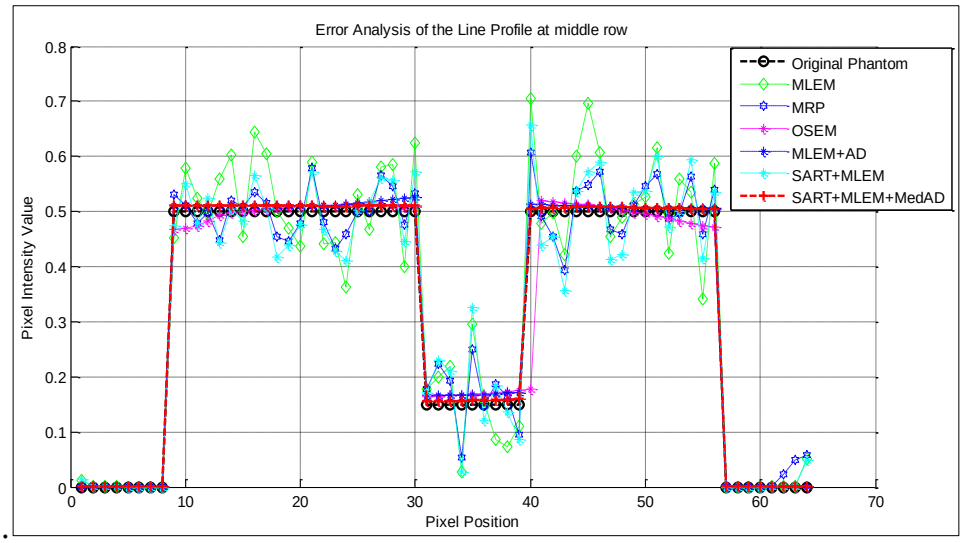

Fig. 4.8: Line Plot of PET Test Phantom using proposed method (SART+MLEM+MedAD) with other methods .

Table 4.2: Performance measures for the reconstructed images for Test case 2

Performance Measures	**MLEM**	**MRP**	**OSEM**	**MLEM+AD**	**SART+MLEM (Proposed method without prior)**	**SART+MLEM+MedAD (Final proposed method with prior)**
SNR	14.5304	19.3744	17.3523	18.8201	18.7362	22.1053
RMSE	0.0775	0.0444	0.0560	0.0473	0.0478	0.0324
PSNR	70.3748	75.2188	73.1967	74.6645	74.5806	77.9498
CP	0.7647	0.9163	0.8901	0.9224	0.9091	0.9870
MSSIM	0.9998	0.9999	0.9999	0.9999	0.9999	1.0000

Test case 3:

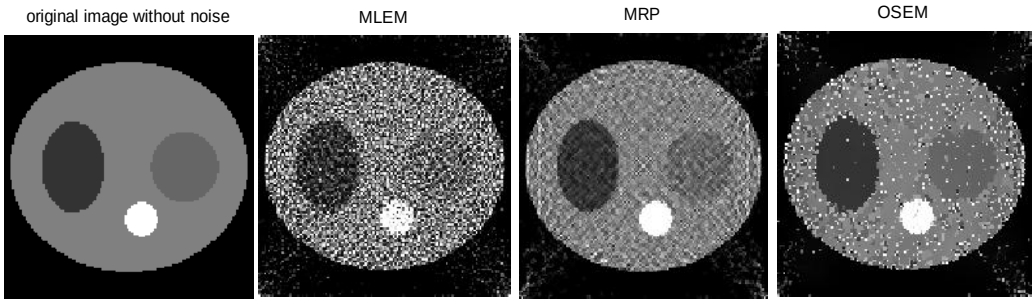

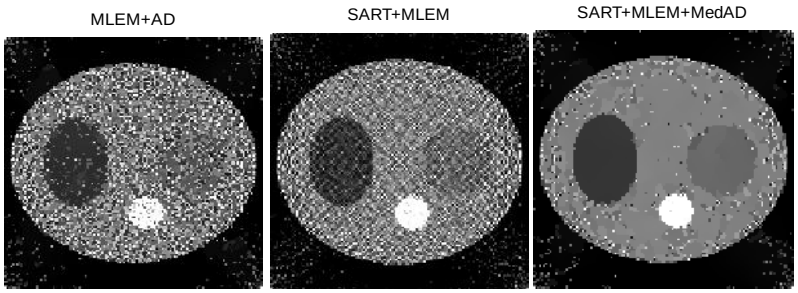

Fig. 4.9: The SPECT test phantom with different reconstruction methods. Projection including 15% uniform Poisson distributed background events.

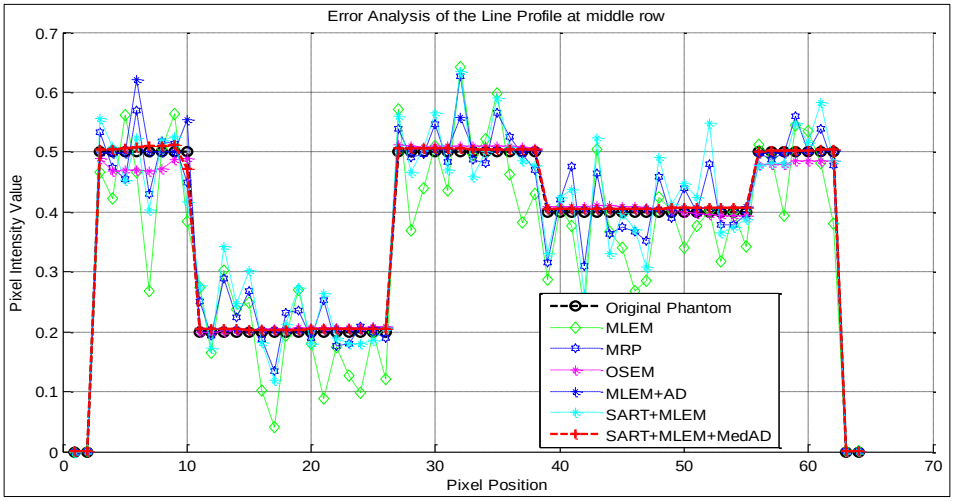

Fig. 4.10: Line Plot of Elliptical Test phantom using proposed method (SART+MLEM+MedAD) with other methods.

Table 4.3: Performance measures for the reconstructed images for Test case 3

Performance Measures	**MLEM**	**MRP**	**OSEM**	**MLEM+AD**	**SART+MLEM (Proposed method without prior)**	**SART+MLEM+MedAD (Final proposed method with prior)**
SNR	13.2096	19.4522	19.0916	19.4477	18.7111	21.4443
RMSE	0.0844	0.0411	0.0429	0.0412	0.0448	0.0327
PSNR	69.6390	75.8816	75.5210	75.8771	75.1405	77.8937
CP	0.7489	0.9322	0.9471	0.9567	0.9248	0.9852
MSSIM	0.9998	1.0000	0.9999	0.9999	1.0000	1.0000

Test case 4

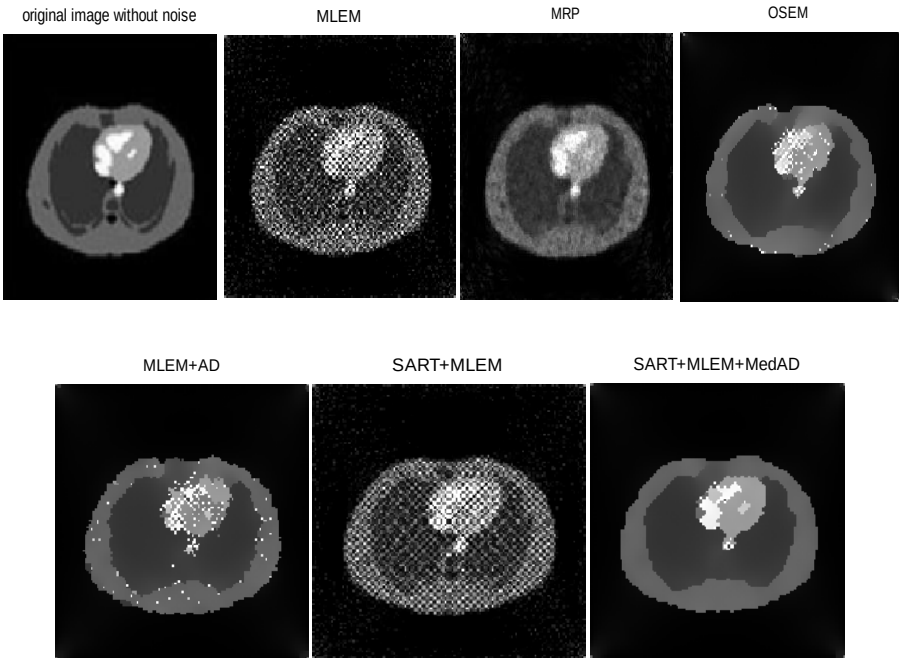

Fig. 4.11: The Real thorax phantom with different reconstruction methods. Projection including 5% uniform Poisson distributed background events.

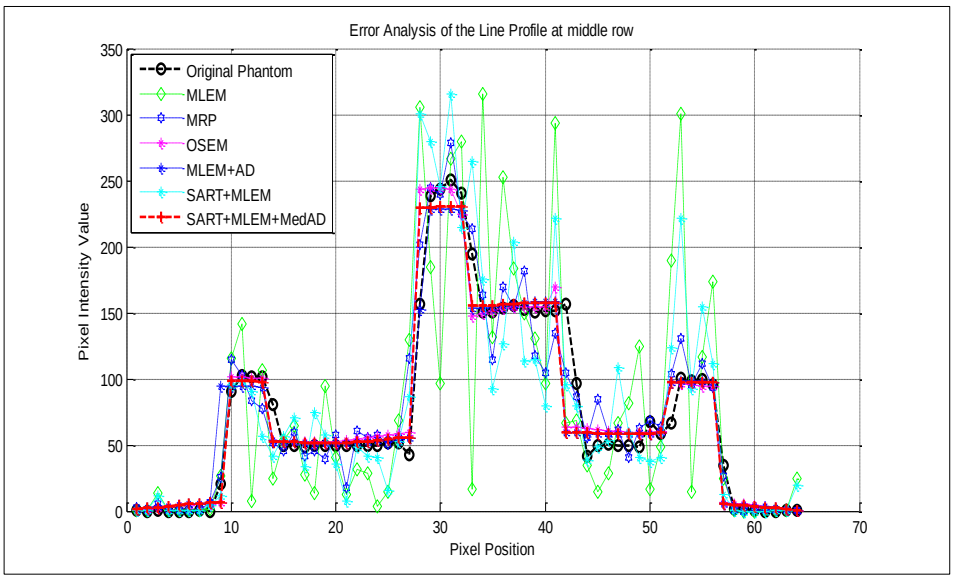

Fig.4.12: Line Plot of standard thorax medical image using proposed method (SART+MLEM+MedAD) with other methods.

Table 4.4: Performance measures for the reconstructed images of Test case 4

Performance Measures	MLEM	MRP	OSEM	MLEM+AD	SART+MLEM (Proposed method with-out prior)	SART+MLEM+MedAD (Final proposed method with prior)
SNR	4.3828	11.0321	9.1262	10.8353	10.9714	11.9768
RMSE	35.8710	16.6831	20.7766	17.0654	16.8000	16.0230
PSNR	17.0699	23.7192	21.8133	23.5225	23.6586	24.650
CP	0.3277	0.7879	0.5618	0.7707	0.7829	0.8102
MSSIM	0.3280	0.5561	0.4910	0.5307	0.5506	0.5550

Fig. 4.5(a) shows the plots of SNR versus the number of iterations for test cases 1-4 respectively. The plots are based on 1000 iterations. From Figure 4.5(a), it is observed that the SNR values associated with the hybrid method is always higher than that produced by other algorithms such as traditional MLEM, MRP, OSEM, and MLEM+AD which indicate that the hybrid framework significantly improves the quality of reconstruction in terms of SNR. Furthermore, it is observed for all the test cases that the proposed method is producing better reconstructed image in 100-150 iterations whereas other methods are taking much higher number of iterations.

Fig. 4.5(b), show that the RMSE values of proposed method is smaller in comparison to other methods which indicate that the proposed method is reconstructed with very less error. Fig. 4.5(c), show that the CP values of proposed method is higher and close to unity in comparison to other methods which indicate that the proposed method is also capable of preserving the fine edges and structures during the reconstruction process. Fig. 4.5(d), show that the MSSIM values of proposed method is higher and closer to unity in comparison to other methods which indicate that in addition to better reconstruction, it also preserves the luminance, contrast and other details of the image during the reconstruction processes. The visual results of the resultant reconstructed images for all the four test cases obtained from different algorithms are shown in Figures 4.4, 4.7, 4.9, and 4.11.

Tables 4.1 – 4.4 show the quantification values of SNRs, RMSEs, PSNRs, CPs, and MSSIMs in for different test cases respectively. The compari-

son tables indicate that proposed reconstruction method produces images with prefect quality than other reconstruction methods in consideration.

Figures 4.6, 4.8, 4.10, and 4.12 shows the error analysis of the line profile at middle row for four different test cases. To check the accuracy of the proceeding reconstructions, line plots for four test cases were drawn, where x-axis represents the pixel position and y-axis represents pixel intensity value. Line plots along the mid-row line through the reconstructions produced by different methods show that the proposed method can recover image intensity effectively in comparison to other methods. Although the MRP can recover image well, even can do better than the proposed algorithm in some place, but it does not preserve the structure of the edges accurately, especially the thin edges and its convergence speed is slow and one can observe that the proposed method does not have this shortcoming. Both the visual-displays and the line plots suggest that the proposed model is preferable to the existing reconstruction methods.

In view of above analysis and discussions for four test cases in consideration it is observed that the proposed hybrid cascaded iterative framework converges very fast, producing the better visual results, having less reconstruction error, higher SNR values, better edge, structure, luminance, and contrast preservation capabilities in comparison to other standard methods in consideration. Furthermore, the proposed method effectively handles the issues of initialization and ill-posedness solution in a better manner. The initialization improves the cost function, which can be exploited to obtain faster convergence than with regularized and un-regularized MLEM. Traditional MLEM performs the worst in both convergence and SNR. Although it seems to match the same performance as by SART+MLEM, it is too slow in convergence. Thus we can say that using SART for initial reconstruction brings the convergence earlier and fetches better results. Similarly for MedAD in regularization term, it significantly enhanced the SNR output. Hence the experimental results show the convergence speed may be a reason to use a hybrid method as a kind of acceleration technique.

4.3.2 An efficient and modified median root prior (MRP) based framework for PET/SPECT Reconstruction Algorithm

Bayesian statistical algorithm plays a significant role in the quality of the images produced by Emission Tomography like PET/SPECT, since they can provide an accurate system model. The major drawbacks associated with this algorithm include the problem of slow convergence, choice of optimum initial point and ill-posedness. To address these issues, in this work a hybrid-cascaded framework for Median Root Prior (MRP) based reconstruction algorithm is proposed. This framework consists of breaking the reconstruction process into two parts viz. primary and secondary. During primary part, simultaneous algebraic reconstruction technique (SART) is applied to overcome the problems of slow convergence and initialization. It provides fast convergence and produce good reconstruction results with lesser number of iterations than other iterative methods. The task of primary part is to provide an enhanced image to secondary part to be used as an initial estimate for reconstruction process. The secondary part is a hybrid combination of two parts namely the reconstruction part and the prior part. The reconstruction is done using Median Root Prior (MRP) while Anisotropic Diffusion (AD) is used as prior to deal with ill-posedness. A comparative analysis of the proposed model with some other standard methods in literature is presented both qualitatively and quantitatively for a simulated phantom and a standard medical image test data. Using cascaded primary and secondary reconstruction steps, yields significant improvements in reconstructed image quality. It also accelerates the convergence and provides enhanced results using the projection data. The obtained result justifies the applicability of the proposed method.

4.3.2.1 Proposed Methods and Models

The proposed hybrid model consists of two parts namely primary reconstruction and secondary reconstruction as shown in Fig.4.13

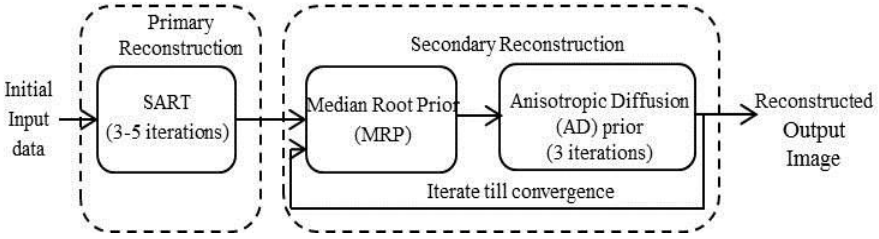

Fig. 4.13: Proposed MRP based hybrid-cascaded framework (Model-2)

The basic SART equation is defined as (Anderson and Kak, 1984):

$$f_j^k = f_j^{k-1} + \frac{\lambda}{\sum_{i=1}^{N} a_{ij}} \sum_{i=1}^{N} \left(\frac{e_j^k}{\sum_{j=1}^{M} a_{ij}} a_{ij} \right) \tag{4.20}$$

Where M is the total number of rays and N is the total number of pixels. λ is the relaxation parameter and error (e_j^k) is calculated in projections using $e_j^k = P_j - p_j^k$,where P is true projections and p_j^k is calculated projections at k^{th} iteration.

A modified MRP algorithm is employed to solve the slow convergence and optimal initialization problem. For this, SART algorithm is implemented in primary reconstruction part and its output is used in secondary reconstruction part as median root prior (MRP) function. To this an extra step is added to Eq. (3) and the modified equation reads for MRP as:

$$f_{OSL,j}^{k+1} = \frac{f_j^{k+1}}{1 + \beta \dfrac{f_{OSL,j}^k - M\left(f_{OSL,j}^k\right)}{M\left(f_{OSL,j}^k\right)}} \tag{4.21}$$

where f_j^k is the value of pixel j after the kth SART step and $f_{OSL,j}^k$ is the same after the k^{th} one-step-late correction. The median filter $M(f_j)$ replaces the value of the j^{th} pixel by the average pixel value contained in the j^{th} pixel neighborhood. Here we use 3×3neighborhood. β is the j^{th} parameter to control the weight of the correction. It is set to 0.25 in this work as it gives better result in the test simulations. Finally the proposed hybrid cascaded framework is as follows:

$$f_{OSL,j}^{k+1,h+1} = f_{OSL,j}^{k+1,h} + \Delta t \sum_{j' \in N_j} \left(C\left(\left| \nabla f_{OSL,j.j'}^{k+1,h} \right| \right) \nabla f_{OSL,j.j'}^{k+1,h} \right), \tag{4.22}$$

where *h* is the diffusion number and diffusion coefficient *C* is defined by Eq. (4.8). For the discretized versions of Eq. (4.22) to be stable, the von Neumann analysis (Rajeev *et. al.,* 2010) shows that we require $\Delta t/(\Delta x)^2 < 1/4$. If the grid size is set to 1, then $\Delta t \leq 1/4$. Therefore, the value of Δt is set to *0.25* for stability of Equation.

- ***The Proposed Algorithm***

a) Primary Reconstruction: Initialize image using SART algorithm

Let the following symbols are used in the primary step of the algorithm:

P = true projections, a = system matrix

g^k = updated image after k^{th} iteration of SART,

p_j^k = calculated projections at k^{th} iteration.

1. Set *k = 0* and chose any random image (zero image density or random image density).
2. Calculate Projections: find projections after kth iterations using updated image: $p_j^k = a_j{}^T * g_i^{(k)}$
3. Calculate Error: Find error in calculated projection using

$$e_j^k = P_j - p_j^k$$

4. Back Projection: update the image after iteration *k*

$$g_i^{(k+1)} = g_i^{(k)} + \frac{\sum_j a_{ij} * \frac{e_j^k}{\sum_{i=1}^{N} a_{ij}}}{\sum_j a_{ij}}$$

5. Put *k = k+1*, repeat for 3-5 iterations. Obtain the final image g_{final} .

b) Secondary Reconstruction: reconstruction using MRP algorithm

Let the following symbols are used in the secondary step of the algorithm:

N_{true} = true projections, G = system matrix

L^k = updated image after kth iteration of SART

N_{calc}^k = calculated projections at kth iteration.

15. Set k = 0 and put $L^0 = g_{final}$

16. Calculate Projections: find projections after kth iterations using updated image : $N_{calc}^k = G^T * L^k$

Error Calculation:-Find error in calculated projection (element-wise division)

$$N_{error}^k = \frac{N_{true}}{N_{calc}^k}$$

Back projection: Back project the error onto image

$$X_{error}^k = G * N_{error}^k$$

17. Normalization:- Normalize the error image(element-wise division)

$$X_{norm}^{k} = \frac{X_{error}^{k}}{\sum_j G_{ij} + \beta\left(\frac{L^k - M\left(L^k\right)}{M\left(L^k\right)}\right)}$$

18. Update:- update the image: $L_m^{k+1} = L^k * X_{norm}^k$

c) Prior: Use AD as prior

19. Set *m = 0* and apply Anisotropic Diffusion

$$L_{m+1}^{k+1} = AD\left(L_m^{k+1}\right)$$

20. Put *m = m+1* and repeat till *m = 3*;
21. Put *k = k+1*, repeat with MRP reconstruction.

In our algorithm, the SNR is monitored during each loop of secondary reconstruction. If the required accuracy for numerical convergence has been achieved then processing is stopped, i.e. when SNR begins to saturate or degrade from any existing value.

4.3.2.2 Results and Discussions

This section presents the qualitative and quantitative analysis of the proposed method with other standard methods for two test cases. First test case is a computer generated Modified Shepp-Logan phantom and another test case is a standard medical thorax images shown in Figure 4.14. The comparative analysis of the proposed method is presented with other standard methods available in literature such as MLEM (Shepp and Vardi, 1982), MLEM+AD (Qian He *et. al.*, 2014), OSEM (Hudson and Larkin, 1994), MRP (Alenius S, Ruotsalainen, 2002) and MRP+AD (Jianhua Yan and Jun Yu, 2007).

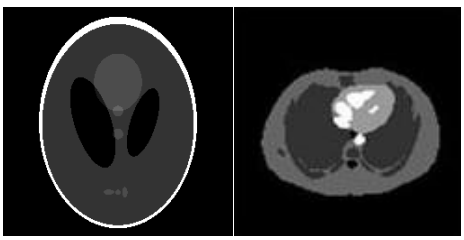

Fig. 4.14: The phantoms used in the simulation study, (a) Modified SheppLogan phantom (64 x 64 pixels), (b) Medical thorax image (128x128 pixels)

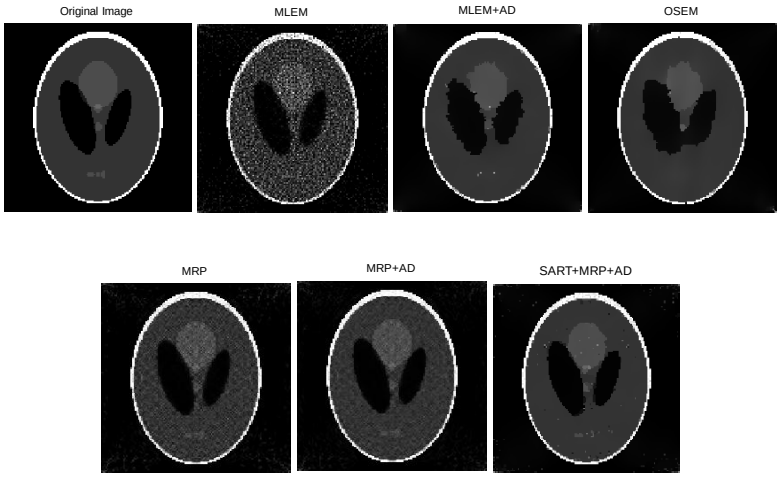

Fig.4.15: The Modified Shepp-Logan phantom with different reconstruction methods. (Projection include 15% uniform Poisson distributed background events)

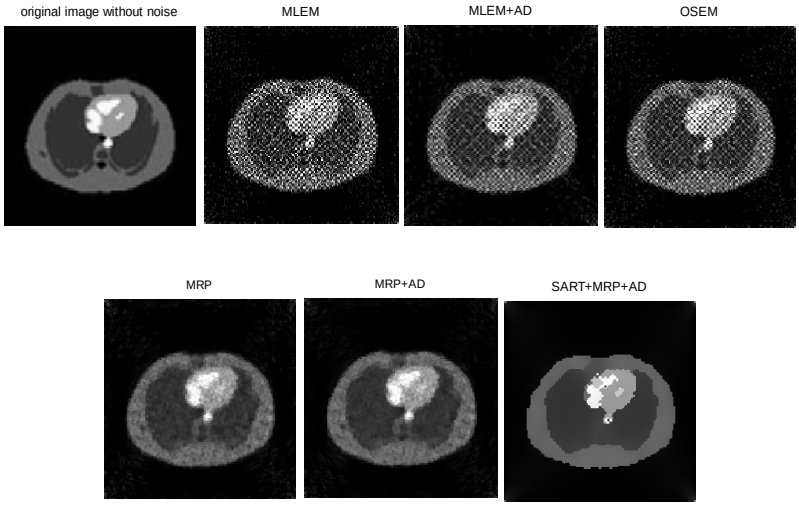

Fig.4.16: The standard thorax medical image with different reconstruction methods. (Projection include 15% uniform Poisson distributed background events)

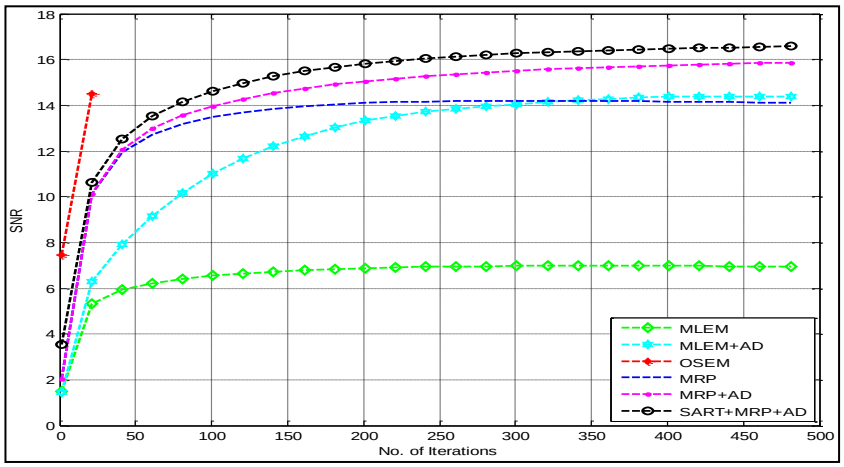

(a)

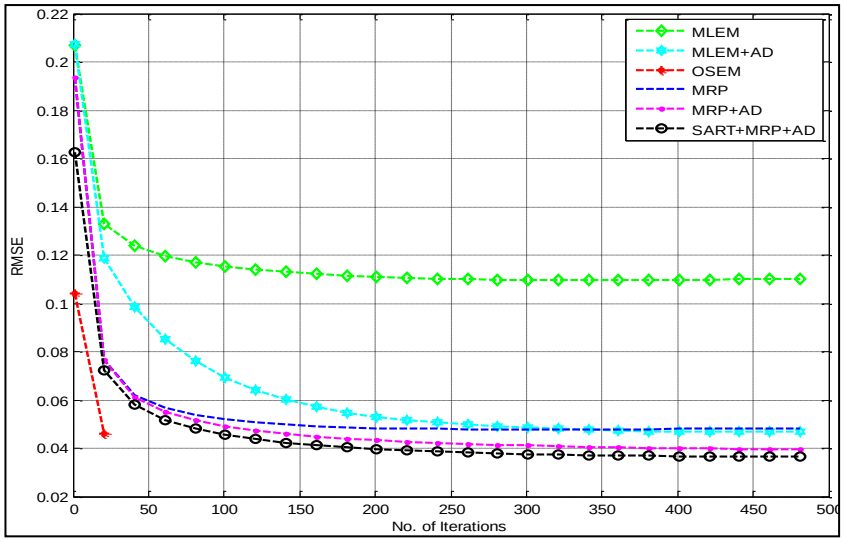
RMSE
No. of Iterations
MLEM
MLEM+AD
OSEM
MRP
MRP+AD
SART+MRP+AD

(b)

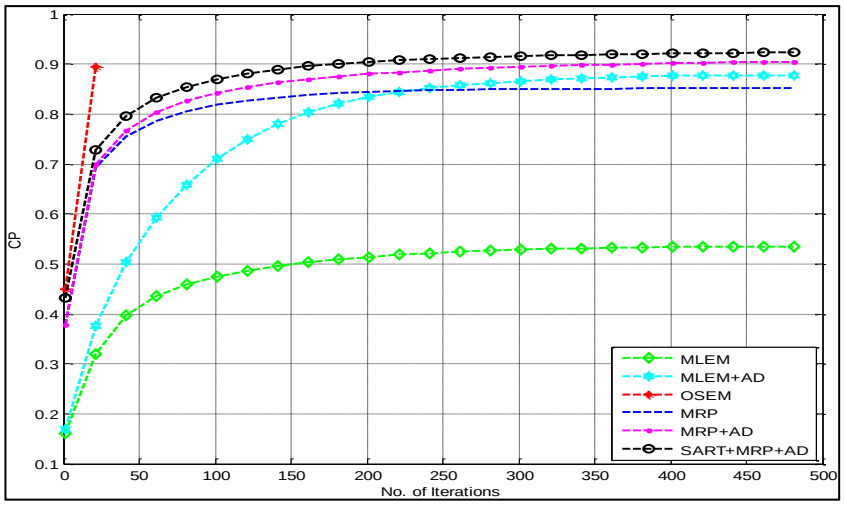
CP
No. of Iterations
MLEM
MLEM+AD
OSEM
MRP
MRP+AD
SART+MRP+AD

(c)

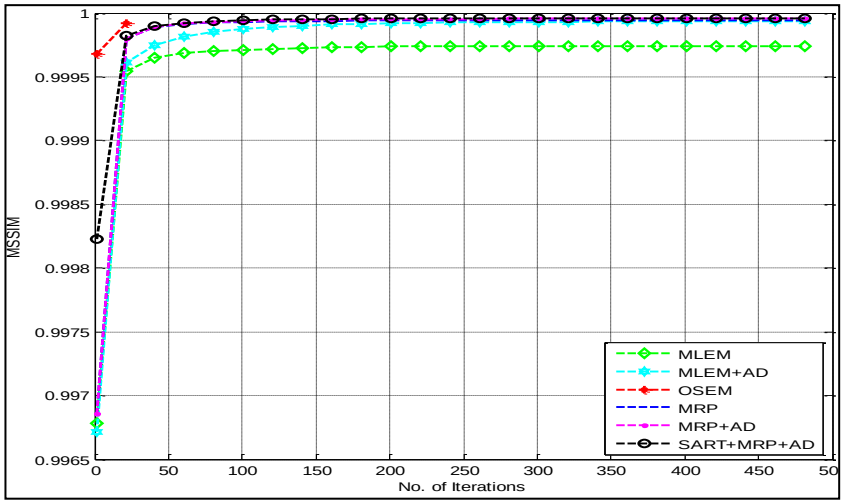
MSSIM
No. of Iterations
MLEM
MLEM+AD
OSEM
MRP
MRP+AD
SART+MRP+AD

(d)

Fig.4.17: The Plots of (a) SNR, (b) RMSE, (c) CP and (d) MSSIM along with No. Iterations for Modified Shepp-Logan Phantom (test case 1).

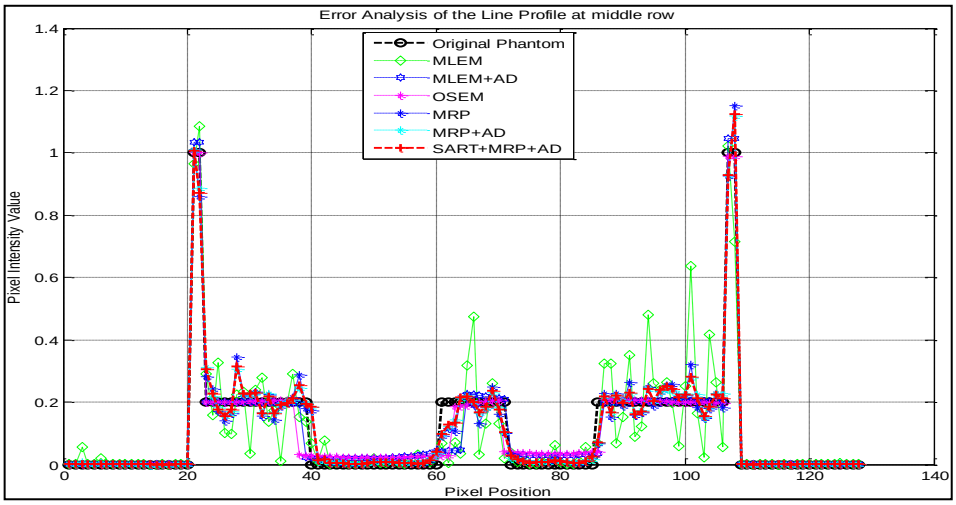

(a)

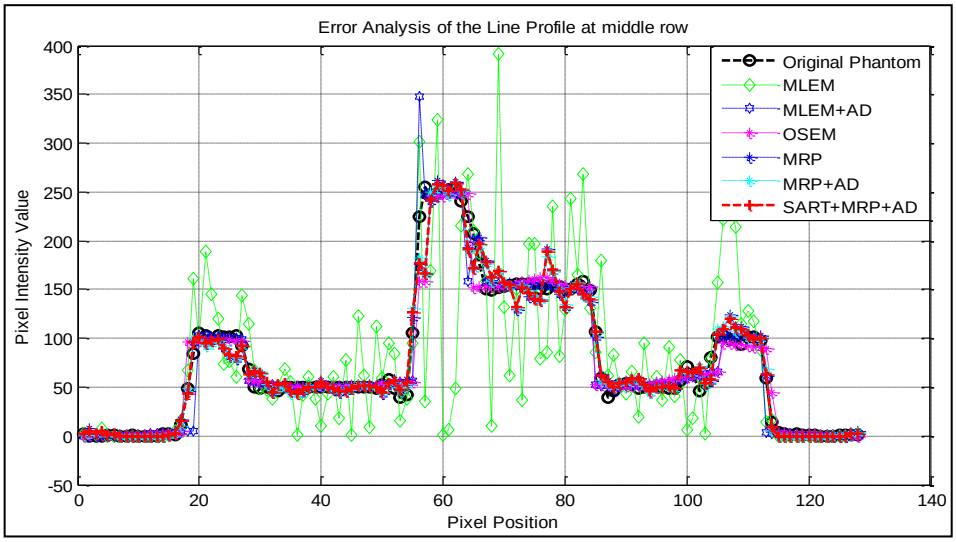

(b)

Fig. 4.18: *Line Plot of (a) Shepp-Logan phantom and (b) standard thorax medical image using proposed and other methods*

Table 4.5: Performance measures for the reconstructed images of Test case 1

	MLEM [8]	**MLEM+ AD [20]**	**OSEM [10]**	**MRP [15]**	**MRP+AD [21]**	**SART+MRP+AD (Proposed Method)**
SNR	7.0027	15.2126	14.9642	14.0646	15.7130	16.3365
RMSE	0.1094	0.0425	0.0438	0.0485	0.0401	0.0374
CP	0.5447	0.9076	0.9105	0.8465	0.9023	0.9200
MSSIM	0.9997	0.9999	0.9999	0.9999	1.0000	1.0000

Table 4.6: Comparison of performance measures for the reconstructed images of Test case 2

	MLEM [8]	MLEM+ AD[20]	OSEM [10]	MRP [15]	MRP+AD [21]	SART+MRP+AD (Proposed method)
SNR	5.0061	13.0371	13.1495	16.5513	16.7531	17.9704
RMSE	33.5103	13.2931	13.1222	8.8699	8.6662	7.5329
CP	0.3831	0.6837	0.7002	0.9364	0.9364	0.9403
MSSIM	0.4291	0.6392	0.6493	0.6832	0.6955	0.7442

The brief description of the various parameters used for generation and reconstruction of the two test cases are mentioned in chapter 2 section performance measures and datasets.

The proposed algorithm was run for 200 to 500 iterations for simulation purposes and the convergence trend of the proposed method and other methods were recorded. However, the proposed and other algorithms converged in less than 500 iterations. Also, this was done to ensure that the algorithm has only single maxima and by stopping at the first instance of stagnation or degradation, we are not missing any further maxima which might give better results. The corresponding graphs are plotted for SNR, RMSE, CP, and MSSIM. The graphs support the fact as shown in Figure 4.17. From these plots, it is clear that proposed method (SART+MRP+AD) gives the better result in comparison to other methods by a clear margin. Using cascaded primary reconstruction and AD in secondary reconstruction brings the convergence much earlier than the usual algorithm. With proposed method, result hardly changes after 300 iterations whereas other methods converge in more than 300 iterations. Therefore, traditional MLEM and MRP perform the worst in both convergence and visual quality. The other methods such as MLEM+AD and MRP+AD take the maximum time to converge. Thus we can say that using SART for primary reconstruction brings the convergence earlier and fetches better results. Similarly for AD in secondary reconstruction, the SNR output is highly enhanced. Further, the proposed model preserves the edges and other radiometric information such as luminance and contrast of the images, the plot correlation parameter (CP) as shown in Figure 4.17.

The visual results of the resultant reconstructed images for both the test cases obtained from different algorithms are shown in Figures 4.15 and 4.16. The experiment reveals the fact that proposed hybrid framework effectively

eliminated Poisson noise and it performs better even at limited number of projections in comparison to other standard methods and has better quality of reconstruction in term of SNRs, RMSEs, CPs, and MSSIMs. Further, from the Figure 4.15 and 4.16, one can see that the proposed method is better capable of preserving the edges and fine structures as well. At the same time, it is also observed that the hybrid cascaded method overcomes the short coming of streak artifacts existing in other iterative algorithms and the reconstructed image is more similar to the original phantom.

Tables 4.5 and 4.6 show the quantification values of SNRs, RMSEs, CPs, and MSSIMs in for both the test cases respectively. The comparison table indicate the proposed reconstruction method produce images with prefect quality than other reconstruction methods in consideration.

Figure 4.18 indicate the error analysis of the line profile at the middle row for two different test cases. To check the accuracy of the proceeding reconstructions, line plots for two test cases were drawn, where x-axis represents the pixel position and y-axis represents pixel intensity value. Line plots along the mid-row line through the reconstructions produced by different methods show that the proposed method can recover image intensity effectively in comparison to other methods. Both the visual-displays and the line plots suggest that the proposed model is preferable to the existing reconstruction methods. From all the above observations, it may be concluded that the proposed model is performing better in comparison to its other counterparts and provide a better reconstructed image.

4.3.3 An OSEM based hybrid-cascaded framework for PET/SPECT Image Re-construction

Expectation Maximization (EM) and the Simultaneous Iterative Reconstruction Technique (SIRT) are two iterative PET/SPECT reconstruction algorithms often used when the data contain a high amount of statistical noise, have been acquired from a limited angular range, or have a limited number of views. A widespread technique to increase the rate of convergence of these types of algorithms has been to perform the correctional updates within subsets of the projection da-

ta. This has given rise to the method of Ordered Subsets EM (OS-EM) and the Simultaneous Algebraic Reconstruction Technique (SART). But, the quality of the reconstructed image with OSEM remains same as EM. Further, it also suffers from the problem of initialization and ill-posedness. On the other hand the quality of reconstructed image produced by SART in first few iterations is better than EM and OSEM but it also suffers from the problem of ill-posedness. To address these aforementioned issues, in this work a hybrid-cascaded framework of OSEM is proposed. This allows us to use more than one algorithm for reconstruction and extract the benefits of each. The proposed model includes two steps: In the primary step, simple algebraic iterative SART method is used as an initial guess for OSEM to deal with the problem of initialization and convergence. The task of primary step will be to provide an enhanced image to secondary step to be used as an initial estimate for reconstruction process. The secondary step is a hybrid combination of two parts namely the OSEM reconstruction and anisotropic diffusion (AD) as a prior. By incorporating a suitable prior knowledge the problem of ill-posedness is addressed. A comparative analysis of the proposed model with some other standard methods in literature is presented both qualitatively and quantitatively for phantom test data sets. The proposed model yields significant improvements in reconstruction quality from the projection data. The obtained result justifies the applicability of the proposed model.

4.3.3.1 Proposed Methods and Models

In this work, a new hybrid-cascaded framework (here referred to as: SART+OSEM+AD) to reduce number of iterations as well as improve the quality of reconstructed images is proposed. This method speedup the process by using a fast algebraic iterative reconstruction algorithm (SART) first and then switch to more precise accelerated version of statistical EM algorithm (OSEM). Additionally, regularization term anisotropic diffusion proposed by Perona and Malik (1990) is combined to maximize the likelihood function. The proposed method solves large computational time, slow convergence as well as ill-conditioned problem of iterative methods. Numerical simulation experience demonstrates that proposed hybrid cascaded reconstruction algorithm is superior to the MLEM, MRP, OSEM and SART alone in performing iterative image re-

construction. Finally, hybrid method is applied to PET/SPECT tomography for obtaining optimal solutions.

The proposed hybrid model consists of two parts namely primary reconstruction and secondary reconstruction as shown in Fig.4.19

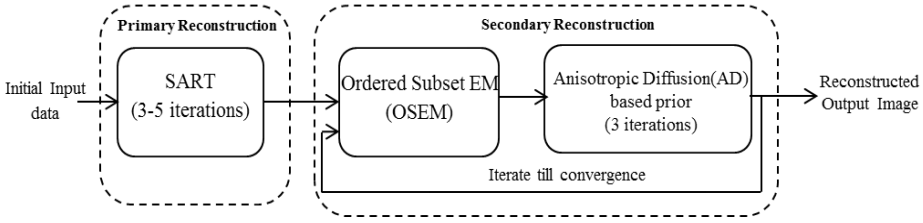

Fig. 4.19: Proposed OSEM based hybrid-cascaded framework (Model-3)

The mathematical model for primary reconstruction phase of the proposed model using SART is given as follows:

$$x_{SART,j}^{k} = x_{j}^{k-1} + \frac{\lambda}{\sum_{i=1}^{N} p_{ij}} \sum_{i=1}^{N} \left(\frac{e_{j}^{k}}{\sum_{j=1}^{M} p_{ij}} p_{ij} \right) \tag{4.23}$$

where M is the total number of rays and N is the total number of pixels. λ is the relaxation parameter and error e_j^k is calculated in projections using $e_j^k = P_j - p_j^k$, where P is true projections and p_j^k is calculated projections at k^{th} iteration.

The output of the k^{th} SART iteration is used as an initial iteration of OSEM and then updating the reconstructed images by nth projections.

Hence, modified OSEM = OSEM (Initial guess image $x^{(0)}$ given by SART):

$$\text{Initial value: } x(i)_j^0 = x_{SART,J}^k \tag{4.24a}$$

$$x(i)_j^{k+1} = x(i)_j^k \left(\frac{1}{\sum_{j \in S_n} a(i,j)} \sum_{j \in S_n} \frac{y(j)a(i,j)}{\sum_{i'=1}^{I} x(i')^{(k)} a(i',j)} \right) \tag{4.24b}$$

for pixels i = 1,2,…, I

where $x(i)_j^{k+1}$ is the value of pixel *j* after the k^{th} iteration of OSEM correction step. Un-regularized image reconstruction in Eq. (4.24) is ill-posed in nature. So, converged OSEM images may be still noisy. There are generally three methods to deal with this problem to suppress the noise. First, one can stop iteration before convergence. However, more iteration may be necessary for recovering image details. Secondly, one can use a post-reconstruction filter to reduce noise. Lastly, one can add a regularizer to Equation (4.24) (e.g. anisotropic diffusion). However, using non-local regularizers for 3D images is computationally very expensive (Chun S. Y. et. al. 2014). In this work, we focus on inbuilt filters within each iteration of OSEM. Recently anisotropic diffusion (AD) is a nonlinear partial differential equation (PDE) based diffusion process (Perona and Malik, 1990) introduced into tomography reconstruction that purports to filter the noise without blurring edges. Overcoming the undesirable effects of linear smoothing filter, such as blurring or dislocating the useful edge information of the images, AD and its variant has been widely used in image smoothing, image reconstruction and image segmentation (Chung Chan et. al., 2009; Zhiguo Gui et. al., 2012; Kazantsev D. et. al., 2012). The anisotropic diffusion (AD) based filter proposed initially by Perona and Malik (1990) reads:

$$\frac{\partial x}{\partial t} = div\left[C\left(|\nabla x|\right).\nabla x\right] \tag{4.25}$$

where x is the image, t is the iteration step, ∇x is the local image gradient and $C(\nabla x)$ is the diffusion function, which is a monotonically decreasing function of the image gradient magnitude, sometimes called the 'edge-preserving' function. The diffusion process is tuned to return large values in the regions with no or small intensity fluctuations and small values in the areas with large intensity variations. This leads to conditional smoothing which encourages intra-region smoothing while preserving the sharp transition between two different regions. The following diffusion coefficient function as proposed by Perona and Malik (1990) was used:

$$C_1\left(|\nabla x|\right) = \frac{1}{1+\left(\frac{|\nabla x|}{Kappa}\right)^a}, \qquad a>1, \tag{4.26}$$

where *Kappa* is a gradient threshold that controls the edge sensitivity of the model. It is a user-specified constant which determines the threshold of the local gradients and controls the edge sensitivity of the filter. Mostly these priors are used at the end of reconstruction when all the data is available for the noise removal and missing/faulty data. Here, by using diffusion on images within the reconstruction process, we get higher SNR values for the final image. Moreover, since noise is tackled in each iteration of secondary reconstruction, the number of iterations required to reach the result are also reduced by great amount and the resulting image is visually enhanced.

$$x_j^{k+1} = x_j^k + \Delta t \sum_{j' \in N_j} \left(C\left(\left| \nabla x_{j,j'}^k \right| \right) \nabla x_{j,j'}^k \right) \qquad (4.27)$$

For the discretized version of Eq. (4.27) to be stable, the von Neumann analysis (William H. Press et. al., 1992) shows that we require $\frac{\Delta t}{(\Delta x)^2} < 1/4$. If the grid size is set to $\Delta x = 1$ then $\Delta t < ¼$ *i.e.(*$\Delta t < 0.25$*)*. Therefore, the value of Δt is set to *0.25* for stability of Equation.

- ***The Proposed Algorithm:***

A. Primary Reconstruction: initialize image using SART algorithm

P = true projections

a = system matrix

x^k = updated image after k^{th} iteration of SART

p_j^k = calculated projections at k^{th} iteration.

1. Set *k = 0* and chose any random image (zero image density or random image density).
2. Calculate Projections: find projections after k^{th} iterations using updated image

$$p_j^k = a_j{}^T * x_i^{(k)} \qquad (4.28)$$

3. Calculate Error:-Find error in calculated projection using

$$e_j^k = P_j - p_j^k \qquad (4.29)$$

4. Back Projection:- update the image after k^{th} iteration using Eq.(4.29)

$$x_j^k = x_j^{k-1} + \frac{\lambda}{\sum_{i=1}^{N} a(i,j)} \sum_{i=1}^{N} \left(\frac{e_j^k a(i,j)}{\sum_{j=1}^{M} a(i,j)} \right) \tag{4.30}$$

5. Put $k = k+1$, repeat for (2-4) iterations. Obtain the final image x_{SART}^{final}.

B. Secondary Reconstruction: reconstruction using OSEM algorithm

X = true projections,

a_{ij} = system matrix,

y^k = updated image after k[th] iteration of secondary reconstruction

x_j^k = calculated projections at k[th] iteration.

6. Set k = 0 and put

$$y^0 = x_{SART}^{final} \tag{4.31}$$

7. Repeat until convergence of $\hat{x}^m$

(a) $x^1 = \hat{x}^m, m = m+1$ (4.32)

(b) For subsets t = 1, 2,….., n

i) Calculate Projections: find projections after k[th] iterations using updated image

$$x(j)^k = \sum_{i=1}^{I} a_{ij}^t \times y^k \text{ , for detectors } j \in S_n \tag{4.33}$$

ii) Error Calculation:-Find error in calculated projection(element-wise division)

$$x_{error}^k = \frac{X}{x_j^k} \tag{4.34}$$

iii) Back projection:-back project the error onto image

$$x(i)_j^{k+1} = x(i)_j^k \left(\frac{1}{\sum_{j \in S_n} a(i,j)} \sum_{j \in S_n} \frac{y(j) a(i,j)}{\sum_{i'=1}^{I} x(i')^{(k)} a(i',j)} \right) \tag{4.35}$$

for pixels i = 1,2,…, I

(c) $X_{error}^k = a_{ij} * x_{error}^k$ (4.36)

8. Normalization:- normalize the error image(element-wise division)

$$X_{norm}^k = \frac{X_{error}^k}{\sum_j a_{ij}} \tag{4.37}$$

9. Update:- update the image

$$y^{k+1} = y^{k} .* X^{k}_{norm} \tag{4.38}$$

C. Prior: Use AD as prior

10. Set m = 0 and apply Anisotropic Diffusion

$$y^{k+1}_{m+1} = AD\left(y^{k+1}_{m}\right) \tag{4.39}$$

Put m = m+1 and repeat till m = 3;

11. Put k = k+1, repeat with OSEM reconstruction.

In our algorithm, the SNR is monitored during each loop of secondary reconstruction. If the required accuracy for numerical convergence has been achieved then processing is stopped, i.e. when SNR begins to saturate or degrade from any existing value.

4.3.3.2 Results and Discussions

For implementation of the proposed method i.e. (SART+OSEM+AD) algorithms Eq. (4.25- 4.30) were used. During step 1 of the proposed method which deals with the problem of initialization to MLEM, SART described by Eq. (4.25) was run for 5-10 iterations and the value of λ was set to 0.0033 for each dataset. Output provided by this step of SART is used as an input to the step 2 of the proposed method. The step 2 uses OSEM and a prior (AD). For experimentation purposes, total number of subsets taken for OSEM algorithm was 8 as it is performing better in comparison to other number of subsets taken. To deal with the problem of ill-posedness of traditional OSEM here in step 2, a hybrid filter as a prior i.e. anisotropic diffusion (AD) filter was used in each step of the traditional OSEM. In step 2 the AD was run for 3 iterations with each OSEM step which is described by Eq. (4.27), for the implementation of step 2 of the proposed algorithm by Eq. (4.30) the value of Δt was set to 1/7 and 0.25 for three computer generated phantoms and standard medical thorax phantom image respectively. For the computation of diffusion coefficient used by Eq. (4.28) and described by Eq. (4.29), the value of threshold parameter *Kappa* was set to 1/100 and 5 for three computer generated phantoms and standard medical thorax phantom image respectively. The whole algorithm was run for 1000 iterations to show the overall convergence pattern though different algorithms converges at

different number of iterations and the proposed one being the faster one. The graphs are plotted for SNR, RMSE, PSNR, correlation parameter (CP), and MSSIM against the number of iterations. This is done to ensure that the algorithm has only single maxima and by stopping at the first instance of stagnation or degradation, we are not missing any further maxima which might give better results. The experiments revealed major observations. The brief description of the three computer generated phantoms and one standard medical thorax phantom image are given in chapter 2: Fig. 4.20, shows the visuals of the test phantoms used for the simulation purposes. These test phantoms are (a) Modified Shepp-Logan phantom (64 x 64 pixels), (b) PET Test phantom (64 x 64 pixels), (c) SPECT Test phantom (64 x 64 pixels), (d) Medical thorax image (128x128 pixels).

(a) (b) (c) (d)

Fig. 4.20: The phantoms used in the simulation study, (a) Modified Shepp-Logan phantom (64 x 64 pixels), (b) PET Test phantom (64 x 64 pixels), (c) SPECT Test phantom (64 x 64 pixels), (d) Medical thorax image (128x128 pixels)

- ***Experimental Analysis and discussions:***

Here, in this work the experimental analysis of the proposed method and other standard methods are presented for four different test cases as follows:

Test case 1:

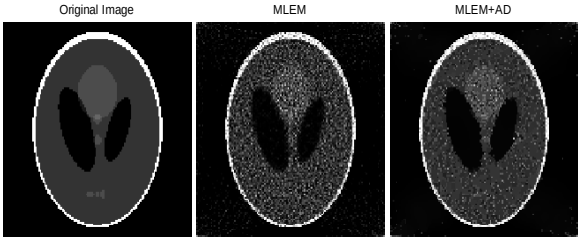

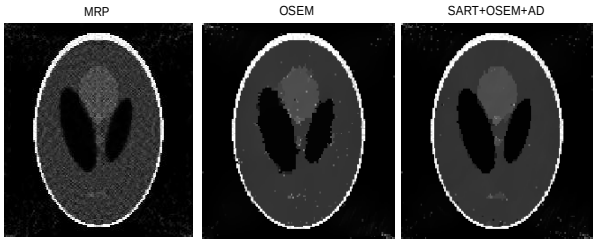

Fig. 4.21: The Modified Shepp-Logan phantom with different reconstruction methods. Projection including 15% uniform Poisson distributed background events.

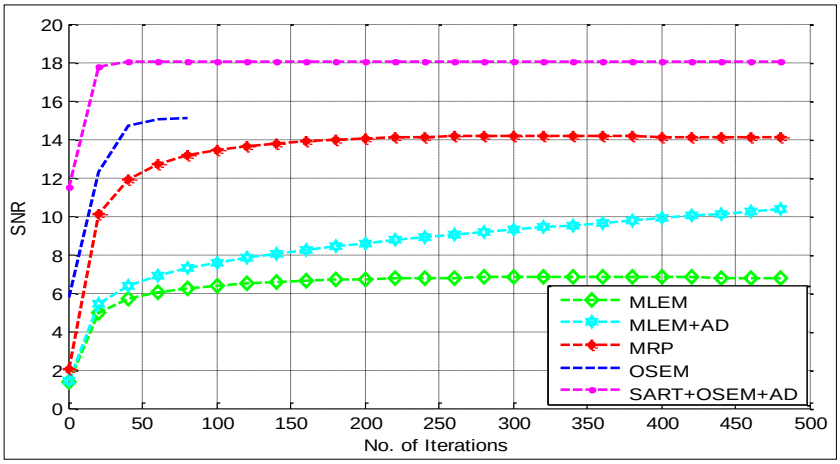

(a)

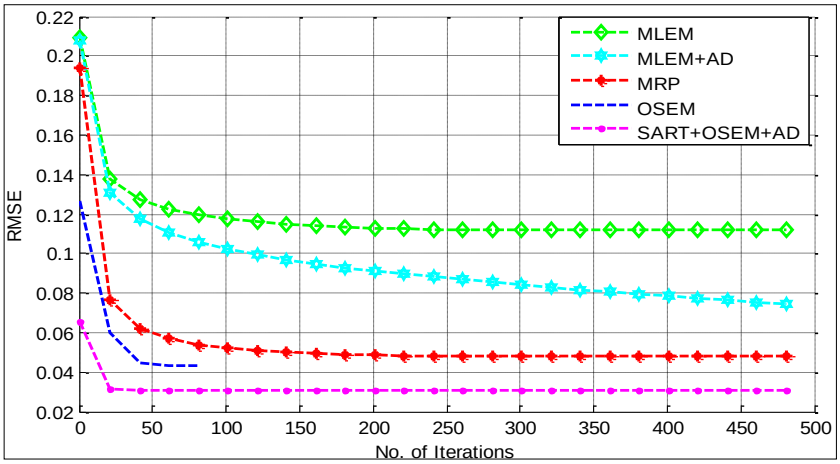

(b)

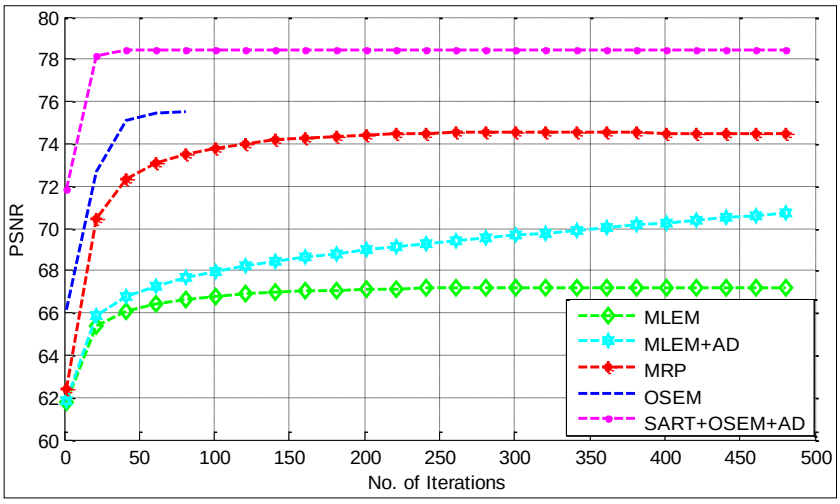

(c)

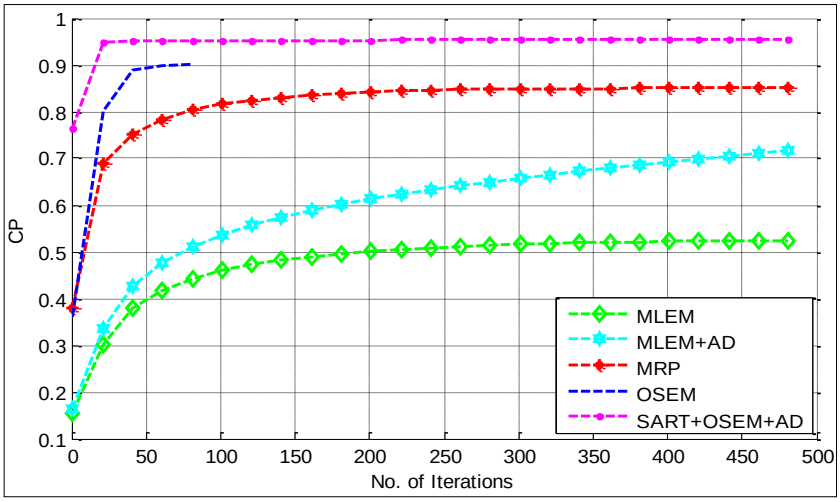

(d)

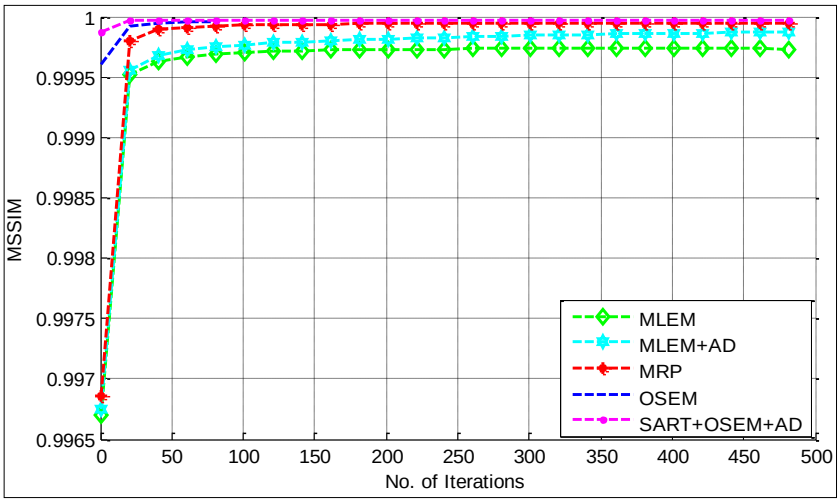

(e)

Fig 4.22: The Plots of (a) SNR, (b) RMSE, (c) PSNR, (d) CP, and (e) MSSIM along with No. of Iterations for different reconstruction methods for Test case 1

Table 4.7: Performance measures for the reconstructed images of Test case 1

Performance Measures	MLEM	MLEM+AD	MRP	OSEM	SART+OSEM+AD (The proposed method)
SNR	6.8231	10.4513	14.1565	15.1511	18.0692
RMSE	0.1117	0.0736	0.0480	0.0428	0.0306
PSNR	67.2038	70.8320	74.5372	75.5319	78.4500
CP	0.5234	0.7218	0.8503	0.9020	0.9532
MSSIM	0.9997	0.9999	0.9999	1.0000	1.0000

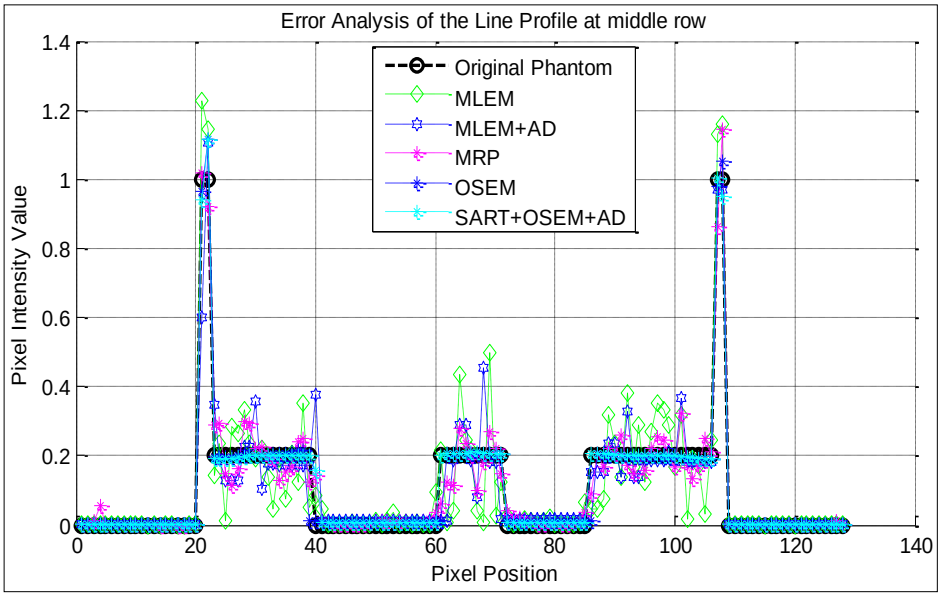

Fig. 4.23: Line Plot of Shepp-Logan Phantom using proposed method (SART+OSEM+AD) with other methods

Test case 2:

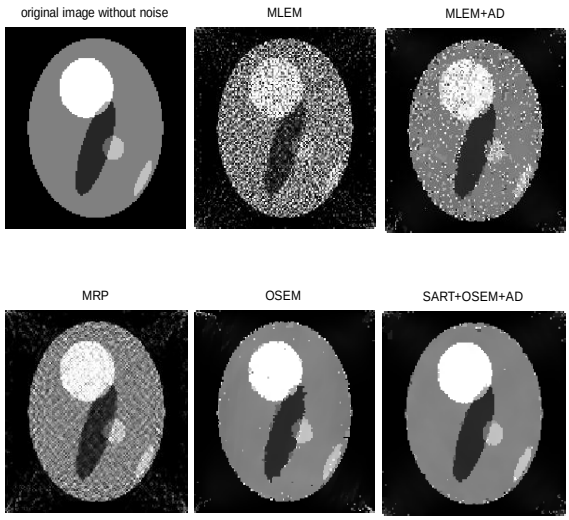

Fig. 4.24: The PET test phantom with different reconstruction methods. Projection including 15% uniform Poisson distributed background events.

Table 4.8: Performance measures for the reconstructed images of Test case 2

Performance Measures	MLEM	MLEM+AD	MRP	OSEM	SART+OSEM+AD (The proposed method)
SNR	13.0047	16.7145	19.2592	18.9275	22.9290
RMSE	0.0924	0.0603	0.0450	0.0467	0.0295
PSNR	68.8491	72.5589	75.1036	74.7719	78.7735
CP	0.6893	0.8608	0.9124	0.9353	0.9870
MSSIM	0.9998	0.9999	0.9999	0.9999	1.0000

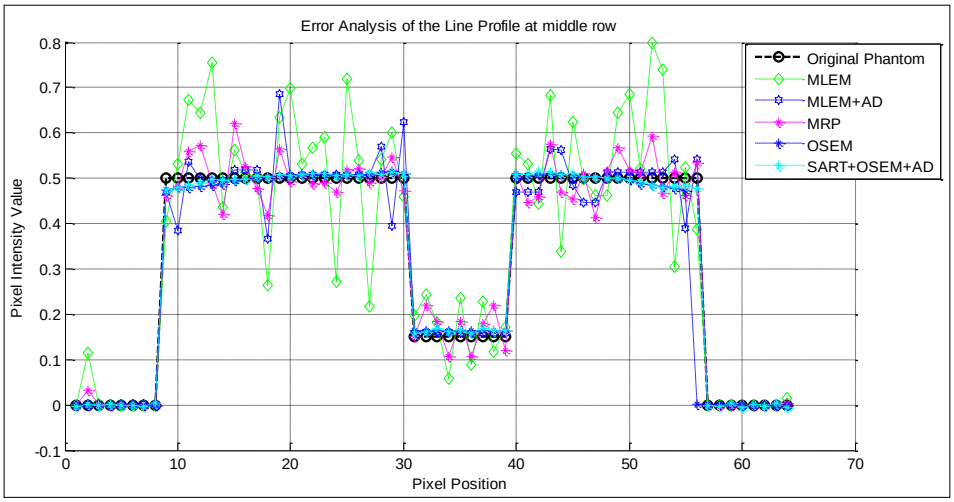

Fig. 4.25: Line Plot of PET Test Phantom using proposed method (SART+OSEM+AD) with other methods

Test case 3:

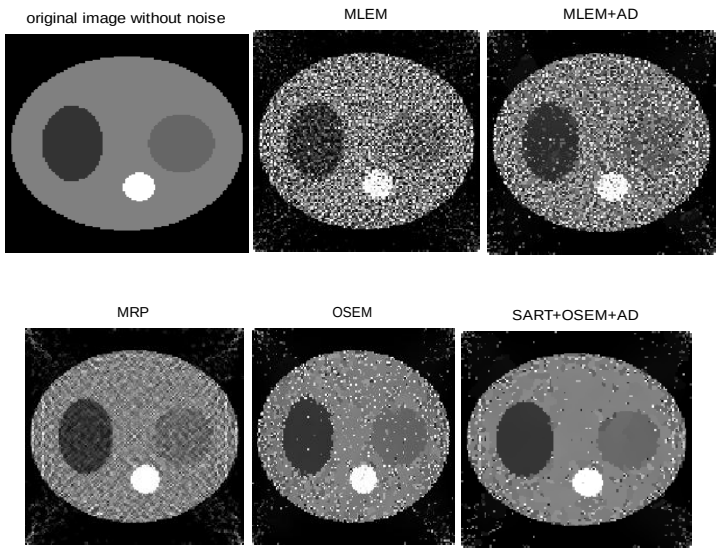

Fig. 4.26: The SPECT elliptical Test Phantom with different reconstruction methods. Projection including 15% uniform Poisson distributed background events.

Table 4.9: Performance measures for the reconstructed images of Test case 3

Performance Measures	MLEM	MLEM+AD	MRP	OSEM	SART+OSEM+AD (The proposed method)
SNR	12.3355	15.9454	19.4039	19.4279	22.7114
RMSE	0.0933	0.0616	0.0414	0.0412	0.0283
PSNR	68.7649	72.3748	75.8333	75.8573	79.1408
CP	0.6962	0.8555	0.9299	0.9533	0.9923
MSSIM	0.9998	0.9999	1.0000	0.9999	1.0000

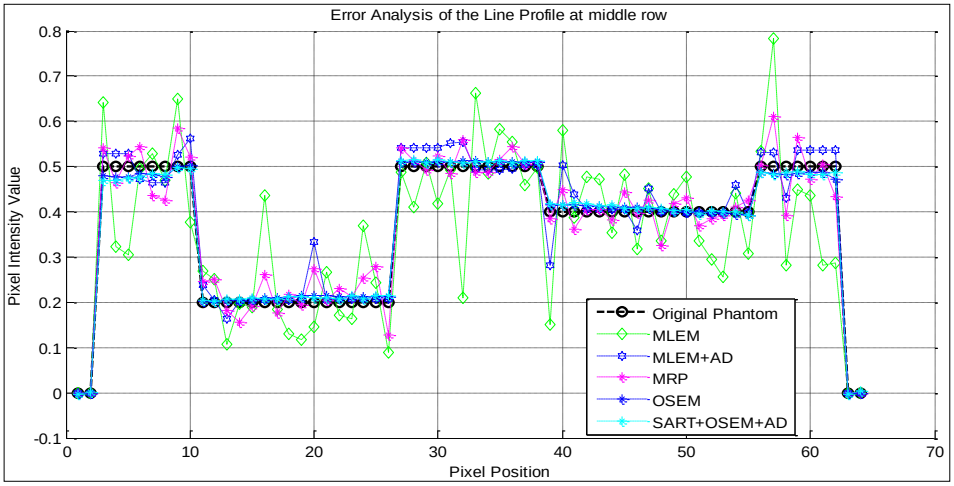

Fig. 4.27: Line Plot of Elliptical Test Phantom using proposed method (SART+OSEM+AD) with other methods

Test case 4

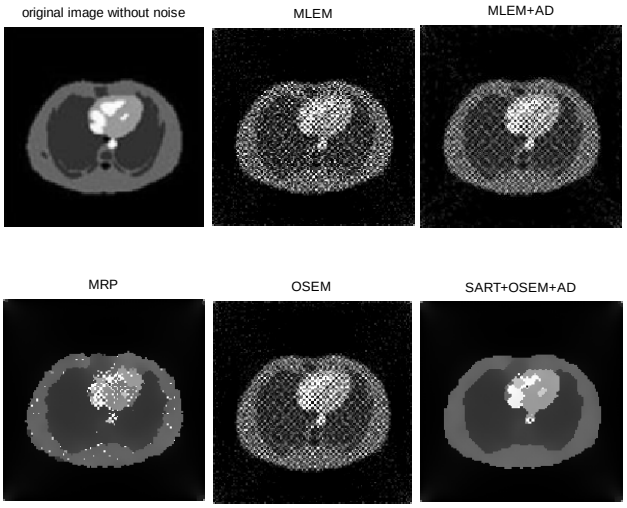

Fig. 4.28: The standard thorax medical image with different reconstruction methods. Projection including 15% uniform Poisson distributed background events.

Table 4.10: Performance measures for the reconstructed images of Test case 3

Performance Measures	MLEM	MLEM+AD	MRP	OSEM	SART+OSEM+AD (The proposed method)
SNR	5.2971	11.1649	13.2200	10.0488	13.6744
RMSE	32.2868	16.4301	12.9683	18.6827	12.3073
PSNR	17.9843	23.8520	25.9071	22.7360	26.3615
CP	0.3007	0.6032	0.8107	0.5324	0.8228
MSSIM	0.4481	0.6378	0.7175	0.5954	0.7502

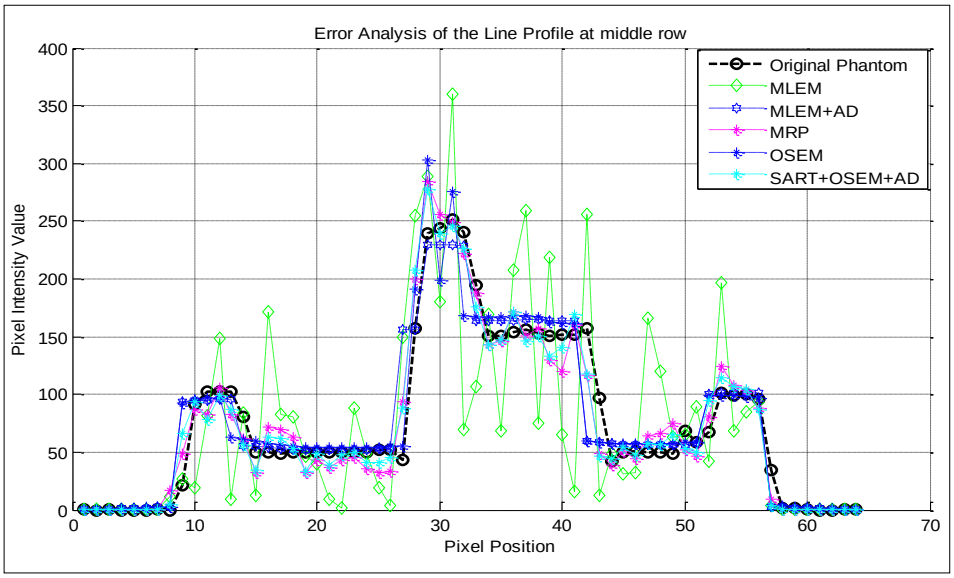

Fig. 4.29: Line Plot of Standard Thorax Test phantom image using proposed method (SART+OSEM+AD) with other methods

The proposed algorithm was run for 1000 iterations for simulation purposes and the convergence trend of the proposed method and other methods were recorded. However, the proposed and other algorithms converged in less than 500 iterations. Also, this was done to ensure that the algorithm has only single maxima and by stopping at the first instance of stagnation or degradation, we are not missing any further maxima which might give better results.

The visual results of the resultant reconstructed images for both the test cases obtained from different algorithms are shown in Figure 4.21,4.24, 4.26, and 4.28. The experiment reveals the fact that proposed hybrid framework effectively eliminated Poisson noise and it performs better even at limited number of projections in comparison to other standard methods and has better quality of reconstruction in term of SNR, RMSE, PSNR, CP, and MSSIM. Further, from the Figure 4.22, one can see that the proposed method is better capable of pre-

serving the edges and fine structures as well. At the same time, it is also observed that the hybrid cascaded method overcomes the short coming of streak artifacts existing in other iterative algorithms and the reconstructed image is more similar to the original phantom.

The corresponding graphs are plotted for SNR, RMSE, PSNR, CP, and MSSIM. The graphs support the fact as shown in Figures 4.22. From these plots, it is clear that proposed method (SART+OSEM+AD) gives the better result in comparison to other methods by a clear margin. Using cascaded primary reconstruction and AD in secondary reconstruction brings the convergence much earlier than the usual algorithm. With proposed method, result hardly changes after 300 iterations whereas other methods converge in more than 300 iterations. Therefore, traditional MLEM perform the worst in both convergence and visual quality. The other methods such as MLEM+AD MRP and OSEM take the maximum time to converge. Thus we can say that using SART for primary reconstruction brings the convergence earlier and fetches better results. Similarly for AD in secondary reconstruction, the SNR output is highly enhanced. Further, the proposed model preserves the edges and other radiometric information such as luminance and contrast of the images, the plot correlation parameter (CP) and mean structure similarity index map (MSSIM) as shown in Fig. 4.22.

Tables 4.7 – 4.10 show the quantification values of SNR, RMSE, PSNR, CP, and MSSIM in for both the test cases respectively. The comparison table indicates the proposed reconstruction method produce images with prefect quality than other reconstruction methods in consideration.

Figures 4.23, 4.25, 4.27, and 4.29 indicate the error analysis of the line profile at the middle row for two different test cases. To check the accuracy of the proceeding reconstructions, line plots for two test cases were drawn, where x-axis represents the pixel position and y-axis represents pixel intensity value. Line plots along the mid-row line through the reconstructions produced by different methods show that the proposed method can recover image intensity effectively in comparison to other methods. Both the visual-displays and the line plots suggest that the proposed model is preferable to the existing reconstruction methods. From all the above observations, it may be concluded that the pro-

posed model is performing better in comparison to its other counterparts and provide a better reconstructed image

4.4 Overall Comparisons of Model 1, Model 2, and Model 3

In this chapter, three different hybrid cascaded framework based on statistical iterative reconstruction algorithms (e.g. MLEM, MRP, and OSEM) have been proposed for PET and SPECT. Their performance analysis are evaluated on computer generated test phantoms and standard thorax real test image and the results are compared with the previous methods proposed by the authors of the papers (Shepp and Vardi, 1982; Alenius S, Ruotsalainen, 2002; Hudson and Larkin, 1994; Qian He *et. al.*, 2014; Zeng GL *et. al.*, 2013; Wang G *et. al.*, 2012). It is observed that the proposed method performs better in terms of visual image quality and different quantitative performance measures.

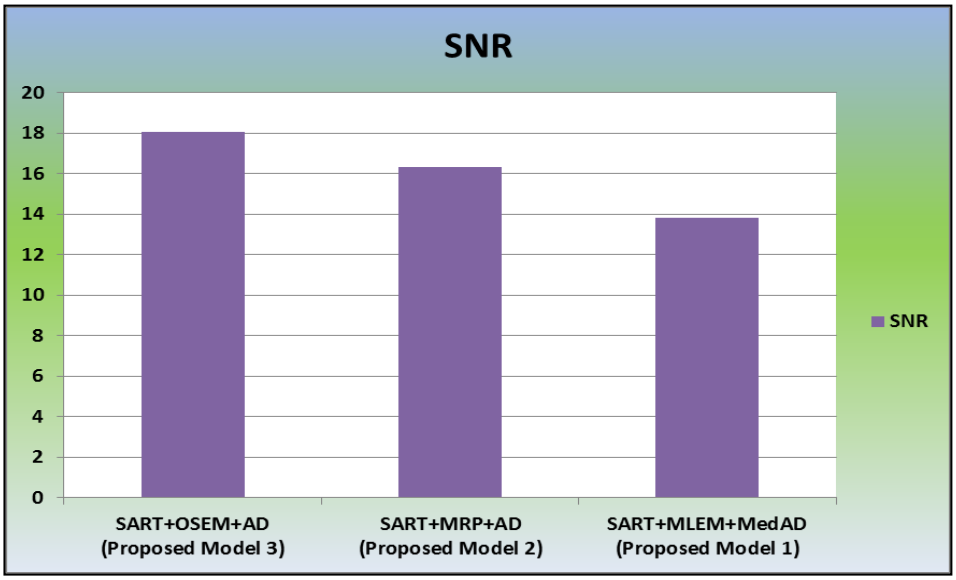

Fig 4.30: The Plots of SNR along with No. of Iterations for different reconstruction algorithms for Test case 1

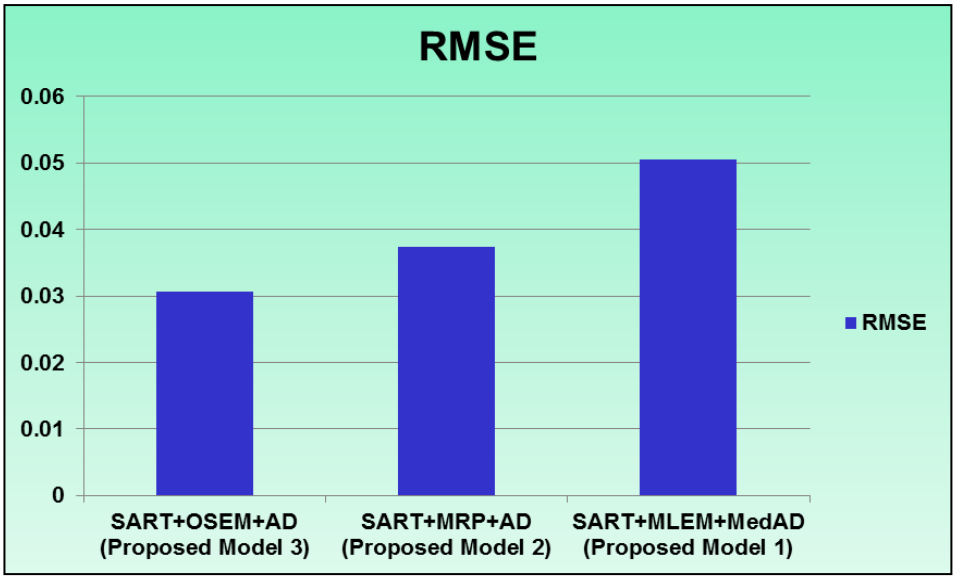

Fig 4.31: The Plots of RMSE along with No. of Iterations for different reconstruction algorithms for Test case 1

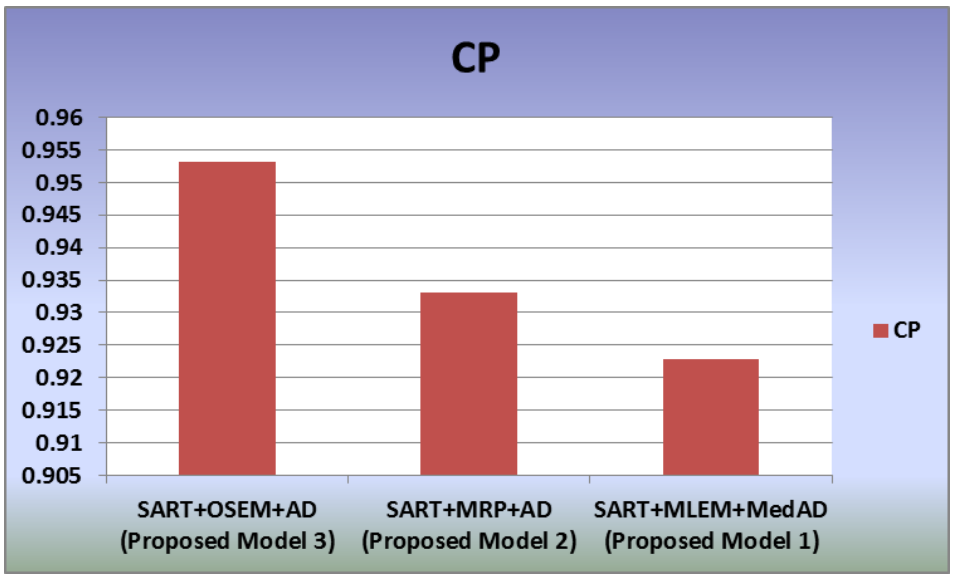

Fig 4.32: The Plots of CP along with No. of Iterations for different reconstruction algorithms for Test case 1

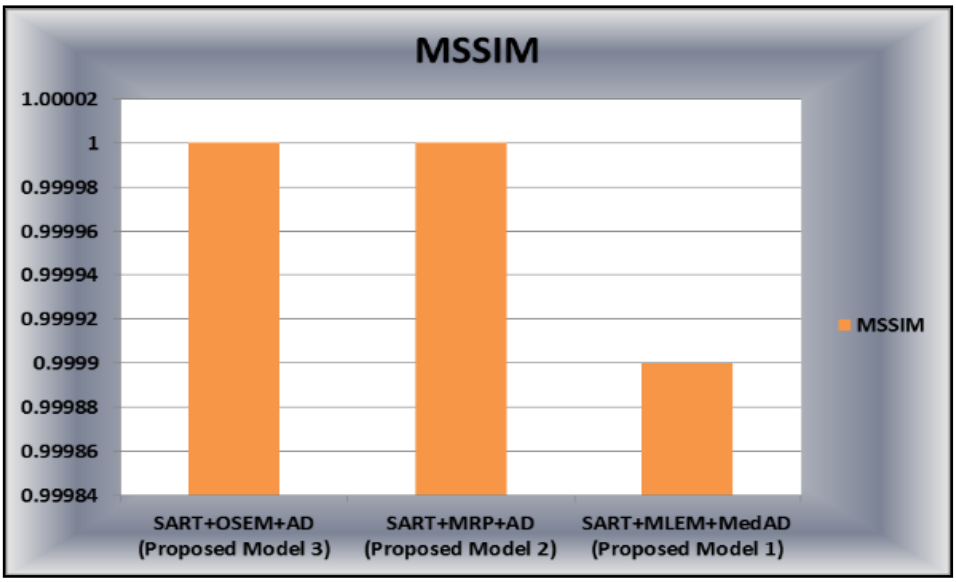

Fig 4.33: The Plots of MSSIM along with No. of Iterations for different reconstruction algorithms for Test case 1

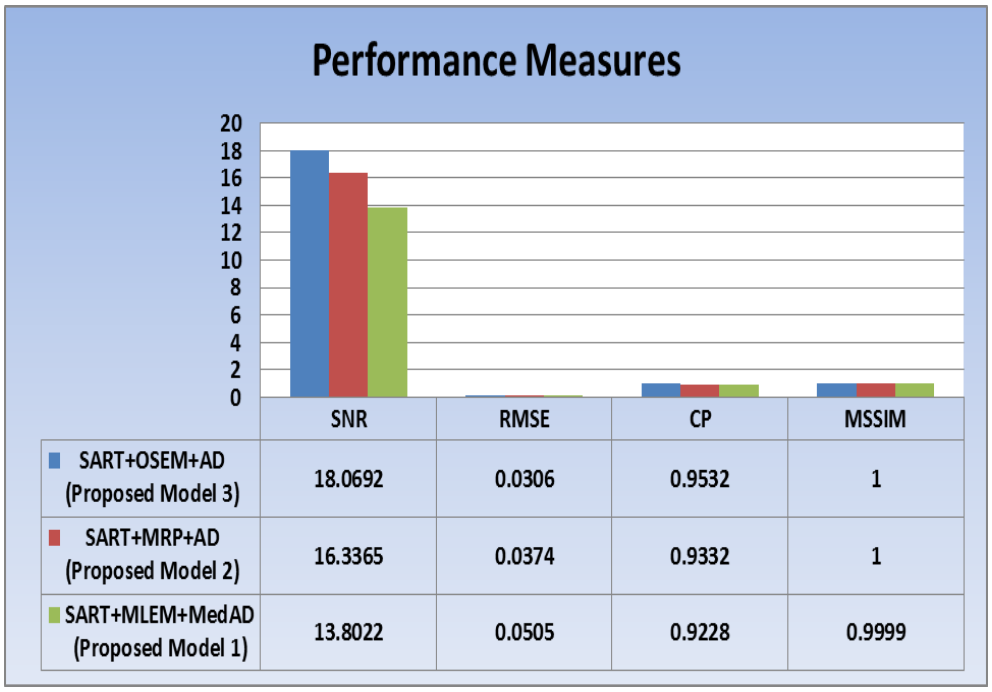

	SNR	RMSE	CP	MSSIM
SART+OSEM+AD (Proposed Model 3)	18.0692	0.0306	0.9532	1
SART+MRP+AD (Proposed Model 2)	16.3365	0.0374	0.9332	1
SART+MLEM+MedAD (Proposed Model 1)	13.8022	0.0505	0.9228	0.9999

Fig 4.34: The overall performance measures of Model 1, Model 2, and Model 3

4.5 Results and Discussions

In this section of the work, results and performance analysis of the three proposed method are presented for three different computer generated PET/SPECT phantoms and one standard medical thorax images both qualitatively and quanti-

tatively. In this simulation study, only two- dimensional (2-D) simulated phantoms were considered. This was because our main aim here is to compare proposed hybrid method with other algorithms and to demonstrate that the proposed method was applicable to different imaging modalities such as PET/SPECT, where 2-D phantoms were sufficient for this purpose.

After critical examination of the comparative results of Model 1, Model 2, and Model 3 as shown in Fig.4.30-4.34. It is found that the OSEM based hybrid-cascaded algorithm which is an accelerated version of MLEM performs better in comparison to other proposed two models with the common projection data. The graphs for SNR, RMSE, correlation parameter (CP), and MSSIM against the number of iterations are plotted in Fig.4.30-4.34. The experiments revealed major observations. It is found that the OSEM based hybrid-cascaded method (accelerated version of MLEM) outperforms with respect to other proposed models on common projection data.

4.6 Conclusion

In this work, three different hybrid-cascaded efficient frameworks for MLEM, MRP and OSEM based SIR reconstruction algorithms were proposed. The proposed frameworks were based on two consecutive modules viz. Primary and secondary. The problems of slow convergence, choice of optimum initial point and ill-posedness are resolved in this framework. During primary part, simultaneous algebraic reconstruction technique (SART) was applied to overcome the problems of slow convergence and initialization. It provided fast convergence and produced good reconstruction results with lesser number of iterations than other iterative methods. The task of primary part was to provide an enhanced image to secondary part to be used as an initial estimate for reconstruction process. The secondary part was a hybrid combination of two parts namely the reconstruction part and the prior part. The reconstruction was done using SIR based methods such as: MLEM, MRP, and OSEM algorithm while anisotropic diffusion (AD) filter is used as prior to deal with ill-posedness. The comparative analysis of the proposed methods with other standard methods was presented for four different test phantoms both qualitatively and quantitatively. The proposed

cascaded framework yield significant improvements in reconstructed image quality. Finally, in the last section of the chapter, after comparison with all three proposed methods, it is concluded that OSEM based hybrid-cascaded framework which is an accelerated version of MLEM performs better with the common projection data in comparison to other two presented methods. Therefore, the use of this proposed method in the image reconstruction of real PET and SPECT studies is possible.